

1 **Dietary propionate induces intestinal oxidative stress via inhibition of**
2 **SIRT3-mediated SOD2 depropionylation**

3 Qian-wen Ding^{1,2}, Zhen Zhang³, Yu Li¹, Hong-liang Liu¹, Qiang Hao¹, Ya-lin Yang³, Einar Ringø²,
4 Rolf Erik Olsen², Jihong Liu Clarke⁴, Chao Ran^{3, #}, Zhi-gang Zhou^{1, #}

5 1 China-Norway Joint Lab on Fish Gastrointestinal Microbiota, Feed Research Institute, Chinese
6 Academy of Agricultural Sciences, Beijing 100081, China

7 2 Norway-China Joint Lab on Fish Gastrointestinal Microbiota, Institute of Biology, Norwegian
8 University of Science and Technology, Trondheim, Norway

9 3 Key Laboratory for Feed Biotechnology of the Ministry of Agriculture, Feed Research Institute,
10 Chinese Academy of Agricultural Sciences, Beijing 100081, China

11 4 NIBIO, Norwegian Institute of Bioeconomy Research, 1431 Ås, Norway

12 # Correspondence and requests for materials should be addressed to Chao Ran (email:
13 ranchao@caas.cn) and Zhi-gang Zhou (email: zhouzhigang03@caas.cn).

14 **Abstract**

15 Propionate is a commonly used preservative in various food and feedstuffs and has been
16 regarded as a food additive without safety concerns. However, we observed that dietary
17 propionate supplementation induced intestinal damage in the context of high fat diet
18 (HFD) in zebrafish. The intestinal damage was attributable to oxidative stress owing to
19 impaired antioxidant capacity, which was caused by compromised SOD2 activity in the
20 intestine. Global lysine propionylation analysis of the intestinal samples showed that
21 SOD2 was propionylated at K132, and further biochemical assays demonstrated that
22 K132 propionylation suppressed SOD2 activity. In addition, SIRT3 could directly
23 interact with SOD2 and played an important role in regulating SOD2 activity via
24 modulating depropionylation, and the enhanced SOD2 propionylation in zebrafish fed
25 high fat plus propionate diet was attributable to reduced SIRT3 expression. Finally, we
26 reveal that intestinal oxidative stress resulting from SOD2 propionylation contributed
27 to the compositional change of gut microbiota, which further deteriorated intestinal
28 oxidative stress independent of SIRT3. Collectively, the results in this study reveal a
29 link between protein propionylation and intestine health, and suggest potential risk of a
30 widely used food preservative in HFD context.

31 **Introduction**

32 Propionic acid (PPA) is a ubiquitous short-chain fatty acid (SCFA), and is a major
33 fermentation product of the enteric microbiome (Koh et al., 2016). As an anti-bacterial
34 compound, propionate is one of the most commonly used preservatives with a

35 maximum allowed concentration up to 0.5% in various foods, such as in cheeses and
36 baked goods, and in animal feedstuffs (Rose, 2013). Propionate inhibits bacterial
37 growth via interrupting enzyme activity and DNA replication (Ng and Koh, 2017).
38 Although propionate is regarded as a food additive without safety concerns (Rose,
39 2013), several studies have indicated that exposure to propionate may cause
40 mitochondrial dysfunction (Matsuishi et al., 1991; Pougovkina, 2016; Stumpf et al.,
41 1980). Furthermore, studies of autism spectrum disorders (ASD) showed that
42 overproduction of propionate resulting from enriched propionate-producing bacteria in
43 individuals with ASD are potentially toxic to the mitochondria (Frye et al., 2015).

44 As a SCFA, propionate crosses the mitochondrial inner membrane and serves as
45 precursor for generation of propionyl-CoA, which could enter the
46 tricarboxylic acid (TCA) cycle for energy metabolism or act as a propionyl-CoA donor
47 for lysine propionylation (Schonfeld & Wojtczak, 2016; Flavin & Ochoa, 1957; Chen
48 et al., 2007; Cheng et al., 2009). Lysine propionylation is a common post-translational
49 modification (PTM) existing in histones of eukaryotic cells, such as 293T cells and
50 yeast (Chen et al., 2007; Cheng et al., 2009; Liu et al., 2009; Zhang et al., 2009). Similar
51 to acetylation and butyrylation, histone propionylation is a marker of active chromatin
52 (Kebede et al., 2017). In contrast to histone propionylation, reports about non-histone
53 propionylation in eukaryotic cells are scarce. Cheng et al. reported the presence of
54 lysine propionylation in three non-histone proteins in 293T cells, i.e., p53, p300, and
55 CREB-binding protein (Cheng et al., 2009). Propionate exhibits mitochondrial toxicity
56 and inhibits mitochondrial respiration in liver and muscle due to significant propionyl-

57 CoA accumulation (Matsuishi et al., 1991). Impaired mitochondrial respiration leads to
58 enhanced production of ROS (Bhatti et al., 2017). Imbalance between ROS generation
59 and clearance accounts for oxidative stress, which leads to mitochondrial dysfunction
60 (Bhatti et al., 2017; Wei et al., 1998; Duchen, 2004; Pieczenik & Neustadt, 2007).
61 Recently, a study phenocopying propionyl-CoA carboxylase deficiency suggested a
62 direct connection between propionyl-CoA accumulation and mitochondrial dysfunction
63 caused by protein propionylation (Pougovkina, 2016). However further identification
64 of propionylated proteins resulting in oxidative stress is insufficient.

65 Studies have demonstrated that gastrointestinal (GI) diseases are associated with
66 ROS and mitochondrial dysfunction. Oxidative stress has important pathogenetic
67 implications for inflammatory bowel disease (IBD) (Palucka, 2007), and enterocytes
68 with abnormal mitochondrial structure have been reported in IBD patients (Novak &
69 Mollen, 2015). The GI tract injury effect of nonsteroidal anti-inflammatory drugs
70 (NSAID) is associated with disruption of mitochondrial structure and function (Rafi,
71 1998; Somasundaram, 1997; Kyle, 2014). Similarly, dextran sodium sulfate (DSS)
72 induces ROS-mediated inflammation in human colonic epithelial cells (Bhattacharyya
73 et al., 2009). On the other hand, antioxidant drugs, such as sulfasalazine, have shown
74 beneficial effects in the treatment of IBD (Bhattacharyya et al., 2014).

75 The intestinal epithelium is prone to oxidative damage induced by luminal
76 oxidants because it locates at the interface between an organism and its luminal
77 environment (Circu & Aw, 2012). In this study, we observed that propionate induced
78 oxidative damage to zebrafish intestine in the context of high fat diet. We revealed a

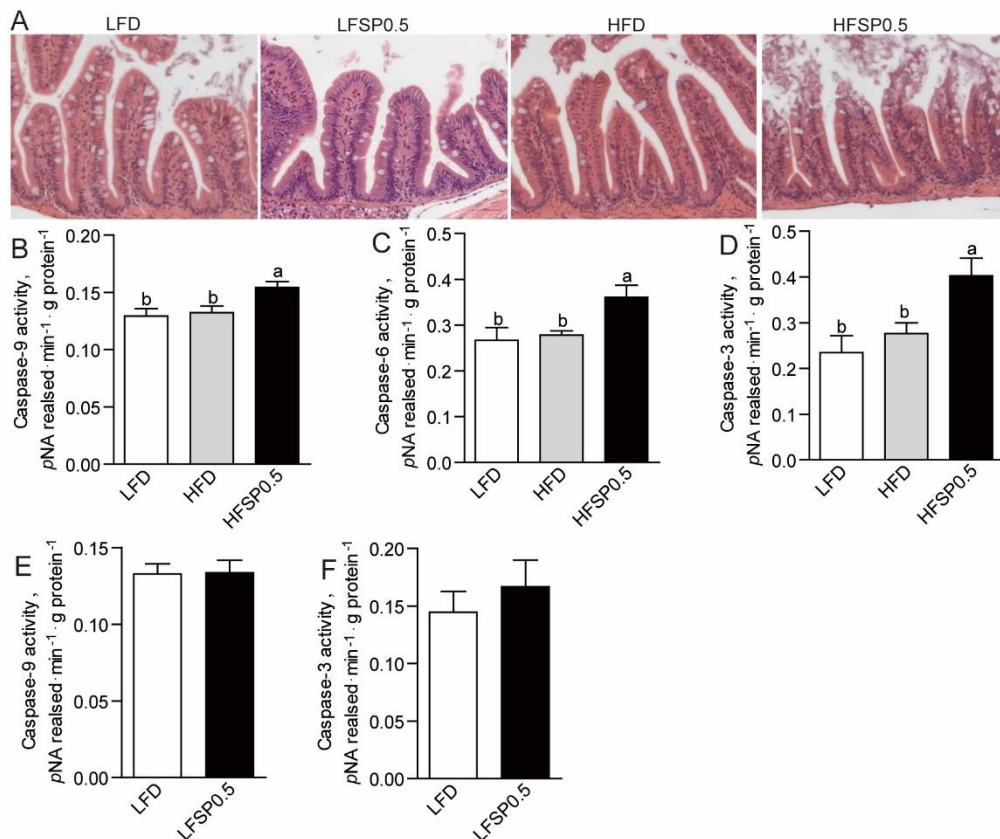
79 mechanism for propionate-induced intestinal oxidative damage that involved
80 propionylation. Superoxide dismutase 2 (SOD2) can be propionylated at the lysine 132
81 site, which suppressed its activity and resulted in oxidative damage in the intestine.
82 Furthermore, we found that the higher propionylation of SOD2 was due to reduced
83 intestinal expression of SIRT3 in zebrafish fed high fat plus propionate diet. In addition,
84 the intestinal microbiota induced by high fat plus propionate diet also contributed to
85 intestinal oxidative stress, in a SIRT3-independent manner.

86 **Results**

87 **Propionate supplementation in high fat diet induces intestinal damage**

88 We established a propionate-feeding model via feeding one-month old zebrafish either
89 low-fat diet (LFD), low-fat diet supplemented with 0.5% sodium propionate (LFSP0.5),
90 high-fat diet (HFD) or high-fat diet supplemented with 0.5% sodium propionate
91 (HFSP0.5) (Supplementary Table 1). Although both oil red staining of liver sections
92 and hepatic TG quantification in zebrafish fed HFSP0.5 diet showed lower lipid
93 accumulation (Supplementary Fig. 1A and 1B), histopathologic analysis of H&E-
94 stained intestine sections showed damage (i.e., breaches in the intestinal epithelium and
95 injury to or loss of intestinal villi) in zebrafish fed HFSP0.5 diet (Fig. 1A). The
96 activation of intestinal caspase-9 (Fig. 1B), caspase-6 (Fig. 1C) and caspase-3 (Fig. 1D)
97 was observed in zebrafish fed HFSP0.5 diet, suggesting that a mitochondrial pathway
98 of apoptosis was activated by the HFSP0.5 diet. Meanwhile, intestinal caspase-8 and
99 caspase-12 activity in zebrafish fed HFSP0.5 diet was similar to that in zebrafish fed

100 HFD (Supplementary Fig. 1C and 1D). However, it is worth noting that sodium
101 propionate supplementation in the context of LFD did not induce damage (Fig. 1A) or
102 the elevation of intestinal caspase-9 and caspase-3 activity (Fig. 1E and 1F), which
103 indicated that sodium propionate becomes a damage-inducing factor in the context of
104 HFD.

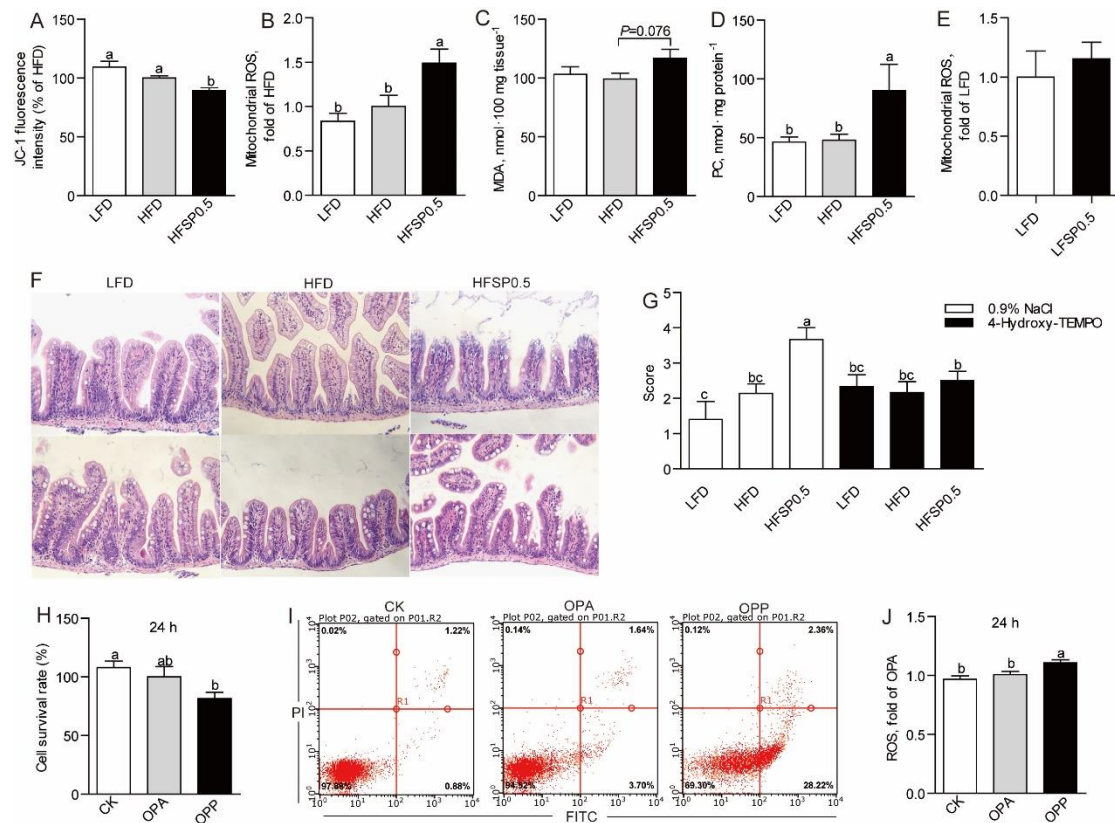


105

Fig. 1 Propionate induces intestinal damage in the context of high fat diet. (A) Representative histopathologic image of H&E-stained intestine sections. (B) Caspase-9, (C) caspase-6 and (D) caspase-3 activity in the intestine of 1-month-old zebrafish fed LFD, HFD or HFSP0.5 diet for 2 wks. (E) Caspase-9 and (F) caspase-3 activity in the intestine of 1-month-old zebrafish fed LFD or LFSP0.5 diet. Values are means \pm SEMs ($n=4\sim6$ biological replicates). Means without a common letter are significantly different, $P<0.05$. LFD, low-fat diet; HFD, high-fat diet; HFSP0.5, high-fat diet supplemented with 0.5% sodium propionate; LFSP0.5, low-fat diet supplemented with 0.5% sodium propionate.

106 **Propionate induces intestinal oxidative stress in zebrafish fed high fat diet**

107 To characterize intestinal damage caused by HFSP0.5 diet, we analyzed the difference
108 in mitochondrial membrane potential (MMP) between zebrafish fed LFD, HFD and
109 HFSP0.5 diet. Compared to zebrafish fed HFD, zebrafish fed HFSP0.5 diet showed
110 significant decrease in intestinal MMP (Fig. 2A), which indicated that HFSP0.5 diet
111 caused mitochondrial dysfunction. HFSP0.5 diet caused oxidative stress in zebrafish
112 intestine, as shown by levels of mitochondrial reactive oxygen species (ROS) (Fig. 1B),
113 malonaldehyde (MDA) (Fig. 2C), and protein carbonyl (PC) content (Fig. 2D), whereas
114 LFSP0.5 diet exerted no effect on mitochondrial ROS (Fig. 2E). Furthermore 4-
115 Hydroxy-TEMPO, a membrane-permeable radical scavenger, alleviated the damage
116 induced by HFSP0.5 diet to intestinal epithelium (Fig. 2F and 2G). We treated the ZF4
117 cell line with a mixture of 150 μ M oleic acid and 50 μ M palmitic acid (OPA), or a
118 mixture of 150 μ M oleic acid, 50 μ M palmitic acid and 50 mM sodium propionate (OPP)
119 to mimic the intestinal damage found with the HFSP0.5 diet. The OPP treatment
120 resulted in 18.5% decrease in cell survival rate (Fig. 2H) and 25.2% increase in cell
121 apoptotic rate (Fig. 2I) at 24 h. OPP exposure resulted in 10.8% increase in cellular
122 ROS at 24 h (Fig. 2J).



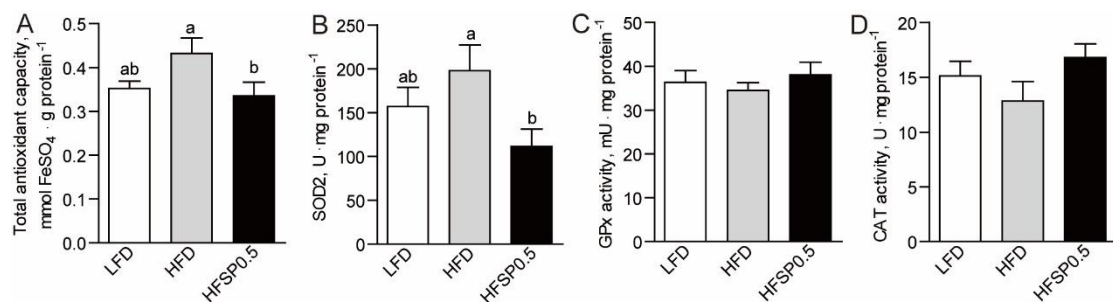
123

Fig. 2 Propionate induces intestinal oxidative stress in the context of high fat diet. (A) The mitochondrial membrane potential in the intestine of 1-month-old zebrafish fed LFD, HFD or HFSP0.5 diet for 2 wks. (B-D) Intestinal biomarkers for oxidative stress in 1-month-old zebrafish fed LFD, HFD or HFSP0.5 diet for 2 wks, including (B) mitochondrial ROS, (C) MDA and (D) PC. (E) Mitochondrial ROS in the intestine of 1-month-old zebrafish fed LFSP0.5 diet. (F) Representative histopathologic images of H&E-stained intestine sections in zebrafish intraperitoneally injected with 4-Hydroxy-TEMPO, a membrane-permeable radical scavenger. (G) Histological score measuring the severity of the intestinal damage of zebrafish intraperitoneally injected with 4-Hydroxy-TEMPO. (H) Cell survival rate and (I) cell apoptotic rate in ZF4 cells treated with a mixture of OPA or OPP for 24 hrs. (J) Cellular ROS in ZF4 cells treated with a mixture of OPA or OPP for 24 hrs. Values are means \pm SEMs, for A-D $n=5$ or 6 biological replicates, for E $n=3$ or 4 biological replicates, for G and H $n=5\sim 12$ biological replicates, for J $n=8$ biological replicates. Means without a common letter are significantly different, $P<0.05$. ROS, reactive oxygen species; MDA, malonaldehyde; PC, protein carbonyl; OPA, mixture of 150 μ M oleic acid and 50 μ M palmitic acid; OPP, mixture of 150 μ M oleic acid, 50 μ M palmitic acid and 50 mM sodium propionate.

124 **Propionate inhibits intestinal total antioxidant capacity in the context of high fat**

125 **diet**

126 Compared with zebrafish fed HFD, zebrafish fed HFSP0.5 diet displayed lower total
127 antioxidant capability (T-AOC) (Fig. 3A) and SOD2 activity (Fig. 3B). However, there
128 was no difference in the activity of other intestinal antioxidant enzymes, such as
129 glutathione peroxidase (GPx) (Fig. 3C) and catalase (CAT) (Fig. 3D) between zebrafish
130 fed HFD and HFSP0.5 diet. These results suggested that inhibition of SOD2 activity
131 induced by HFSP0.5 diet mainly contribute to impaired T-AOC and oxidative stress.



132

Fig. 3 Propionate inhibits intestinal total antioxidant capacity in the context of high fat diet. (A) Intestinal total antioxidant capability in 1-month-old zebrafish fed LFD, HFD or HFSP0.5 diet for 2 wks. (B-D) Intestinal antioxidant enzymes in 1-month-old zebrafish fed LFD, HFD or HFSP0.5 diet for 2 wks, including (B) SOD2, (C) GPx and (D) CAT. Values are means \pm SEMs ($n=5$ or 6 biological replicates). Means without a common letter are significantly different, $P<0.05$. SOD2, superoxide dismutase 2; GPx, glutathione peroxidase; CAT, catalase.

133 Propionate induces SOD2 propionylation at 132 lysine site

134 Contrary to lower SOD2 activity, the protein level of intestinal SOD2 in zebrafish fed
135 HFSP0.5 diet was identical to that in zebrafish fed HFD (Fig. 4A and 4B). Since
136 propionate serves as precursor for generation of propionyl-CoA (Schonfeld & Wojtczak,
137 2016), it seems reasonable to propose that the difference in SOD2 activity between the
138 HFSP0.5 group and the HFD group may involve posttranslational propionylation of
139 SOD2.

140 Global lysine propionylation performed via HPLC-MS/MS-based proteomics
141 technology showed that SOD2 was the only propionylated antioxidant enzyme in

142 mitochondria (Supplementary Fig. 2). The results showed that SOD2 was propionylated
143 at the 132 lysine site (K132) (Fig. 4A, 4C and 4D). The propionylation of SOD2 K132
144 was enhanced by exposure of OPP in ZF4 cells (Fig. 4E). Compared with zebrafish fed
145 LFD, zebrafish fed HFD and HFSP0.5 diets showed a lower mRNA level of the PCCa
146 subunit (Fig. 4F). Moreover, zebrafish fed HFSP0.5 diet showed a lower mRNA level
147 of the PCCb subunit compared with zebrafish fed LFD and HFD (Fig. 4G), which
148 indicated that propionate metabolism in the intestine may be disturbed by HFD and
149 HFSP0.5 diets.

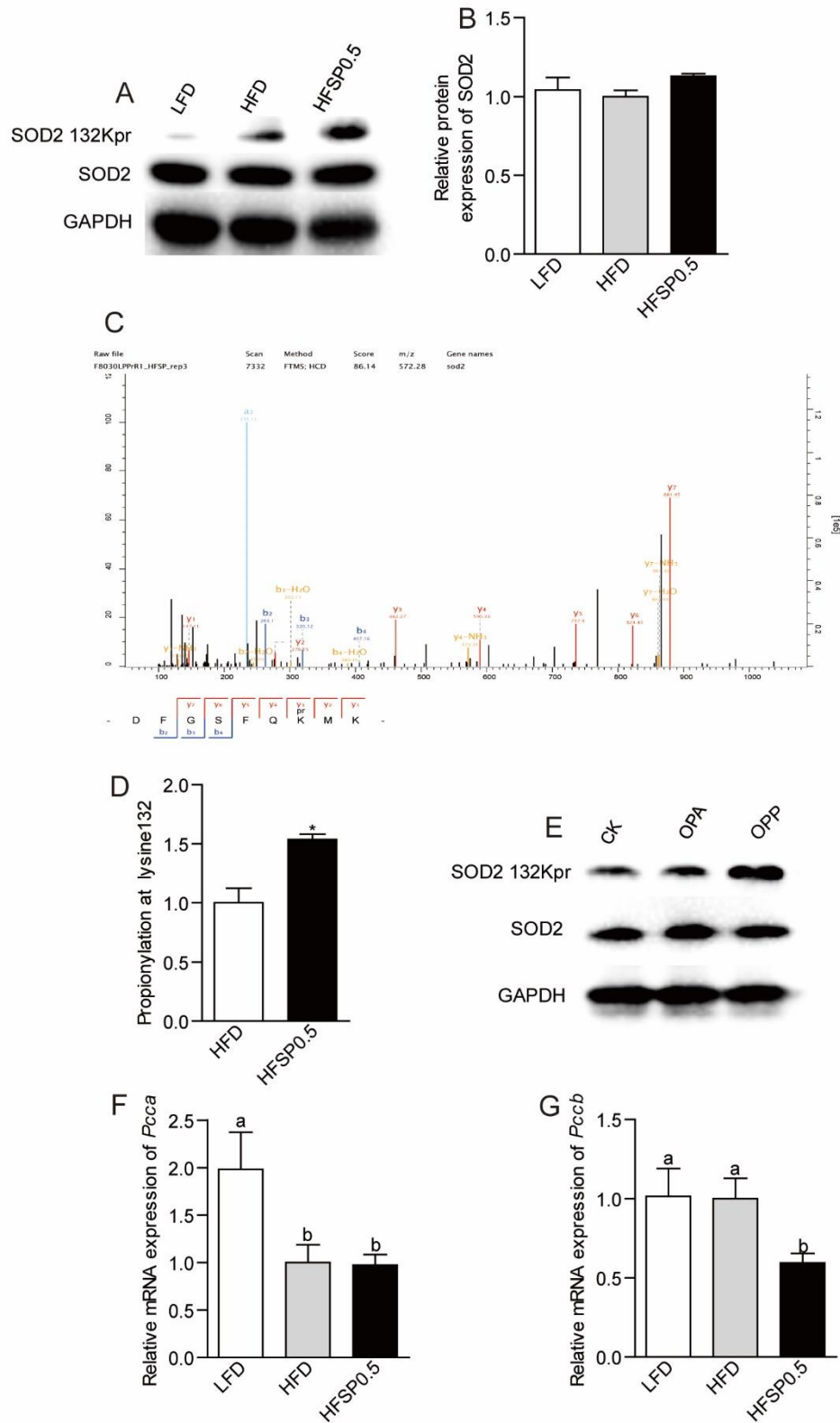


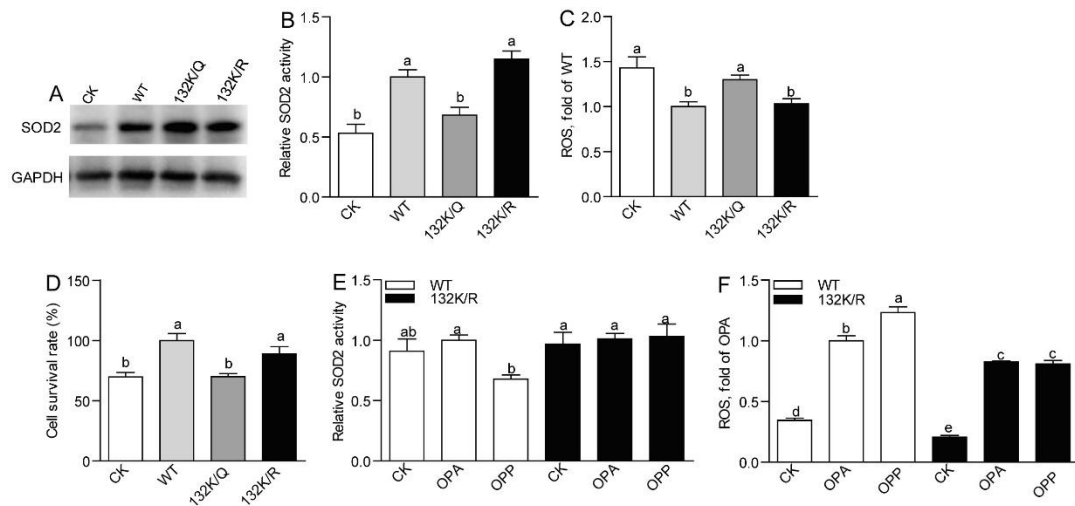
Fig. 4 Propionate contributes to SOD2 propionylation at 132 lysine site in the context of high fat diet. (A) A representative western blotting showing patterns of intestinal SOD2 expression and SOD2 propionylation at the 132 lysine site. (B) Quantification of intestinal SOD2 protein level in zebrafish fed LFD, HFD or HFSP0.5 diet for 2 wks. (C) Tandem mass spectrometry from SOD2 demonstrates propionylated lysine 132 *in vivo*. (D) Quantification of intestinal SOD2 propionylation

at the 132 lysine site in zebrafish fed HFD or HFSP0.5 diet for 2 wks. (E) A representative western blotting showing patterns of SOD2 expression and SOD2 propionylation at the 132 lysine site in ZF4 cells treated with OPA or OPP. (F-G) The mRNA expression of genes encoding subunits of intestinal PCC, an enzyme catalyzing the carboxylation of propionyl-CoA, in zebrafish fed HFD or HFSP0.5 diet for 2 wks. Values are means \pm SEMs, for B and D $n=2$ or 3 biological replicates; for F and G $n=6$ biological replicates. Means without a common letter are significantly different, $P<0.05$. * $P<0.05$, ** $P<0.01$. OPA, mixture of 150 μ M oleic acid and 50 μ M palmitic acid; OPP, mixture of 150 μ M oleic acid, 50 μ M palmitic acid and 50 mM sodium propionate; PCC, propionyl-CoA carboxylase.

151 **SOD2 propionylation at 132 lysine site accounts for cellular ROS increase.**

152 To determine whether propionylation at K132 compromises the activity of SOD2, we
153 generated plasmid expressing mutated zebrafish SOD2 in which K132 was substituted
154 by arginine (R, conserves the positive charge) or glutamine (Q, mimics lysine
155 propionylation) (K132R/Q), and transfected the plasmid into ZF4 cells under SOD2
156 knockdown state. *SiRNA* (mixture of *Sod2-1* and *Sod2-3*) targeting SOD2 was used to
157 reduce its expression in ZF4 cells and scrambled *siRNA* was used as a negative control
158 (Supplementary Fig. 3A, Supplementary Table 3). Results showed that overexpression
159 of WT SOD2 and SOD2 K132R/Q compensated the protein level of SOD2 (Fig. 5A).
160 Compared with the cells transfected with WT SOD2, ZF4 cells transfected with SOD
161 K132R mutant showed similar SOD2 activity, ROS level and cell viability (Fig. 5B-
162 5D), while cells transfected with SOD2 K132Q mutant displayed decreased SOD2
163 activity (Fig. 5B), increased ROS level (Fig. 5C) and lower cell viability (Fig. 5D).
164 These results indicated that propionylation in K132 compromises the enzymic activity
165 of SOD2, leading to enhanced ROS. Moreover, overexpression of SOD2 K132R in ZF4
166 cells prior to OPP treatment maintained SOD2 activity (Fig. 5E) and prevented cellular
167 ROS elevation (Fig. 5F) when compared to overexpression of WT SOD2, supporting

168 that K132 propionylation induced reduction of SOD2 activity was the main cause of
169 enhanced ROS under high lipid plus propionate conditions. Collectively, these results
170 indicated that propionylation of SOD2 at K132 inhibits SOD2 activity and accounts for
171 cellular ROS accumulation.



172

Fig. 5 SOD2 propionylation at 132 lysine site accounts for cellular ROS increase. (A) A representative western blotting showing that overexpression of WT SOD2 and SOD2 K132R/Q compensated SOD2 level in ZF4 cells. (B) SOD2 activity, (C) ROS level and (D) cell survival rate in ZF4 cells transfected with WT SOD2 or SOD K132R/Q mutants. (E) SOD2 activity and (F) ROS level in ZF4 cells treated with OPA or OPP, which were transfected with WT SOD2 and SOD2 K132R in advance. Values are means \pm SEMs ($n=4-8$ biological replicates). Means without a common letter are significantly different, $P<0.05$. OPA, mixture of 150 μ M oleic acid and 50 μ M palmitic acid; OPP, mixture of 150 μ M oleic acid, 50 μ M palmitic acid and 50 mM sodium propionate.

173 Inhibition of SIRT3 promotes SOD2 propionylation

174 Recent studies identified that the sirtuin family of deacetylases have depropionylation
175 activity (27 Bheda et al., 2011). To identify which sirtuin is involved in the regulation
176 of SOD2 K132 propionylation, we evaluated the expression of sirtuins in zebrafish
177 intestine. Results showed that the expression of intestinal sirtuin 3 (SIRT3) was reduced
178 in zebrafish fed HFSP0.5 diet when compared with those fed HFD (Fig. 6A-6C). We
179 next examined whether SIRT3 could interact with SOD2 in physiological conditions

180 via immunoprecipitation with intestine lysate. Results showed that SIRT3 could be
181 immunoprecipitated with SOD2 antibody (Fig. 6D). Moreover, exposure of OPP
182 reduced mRNA expression of *Sirt3* in ZF4 cells (Fig. 6E-6G). To identify whether
183 SIRT3 reduction is associated with propionylation of intestinal SOD2 at the K132 site,
184 we knocked down *Sirt3* with *siRNA* (mixture of *Sirt3*-1, *Sirt3*-2 and *Sirt3*-3) in ZF4
185 cells (Supplementary Fig. 3B, Supplementary Table 3) and detected propionylation of
186 SOD2 at the K132 site via western blot. Results showed that the knockdown of *Sirt3*
187 increased propionylation of SOD2 at K132 (Fig. 6H). In agreement with increased
188 propionylation of SOD2 at K132 in *Sirt3* KD ZF4 cells, the activity of SOD2 (Fig. 6I)
189 and cell viability (Fig. 6J) were significantly reduced. Together, these results indicated
190 that SIRT3 can directly interact with SOD2 and plays an important role in regulating
191 SOD2 activity via modulating propionylation at K132.

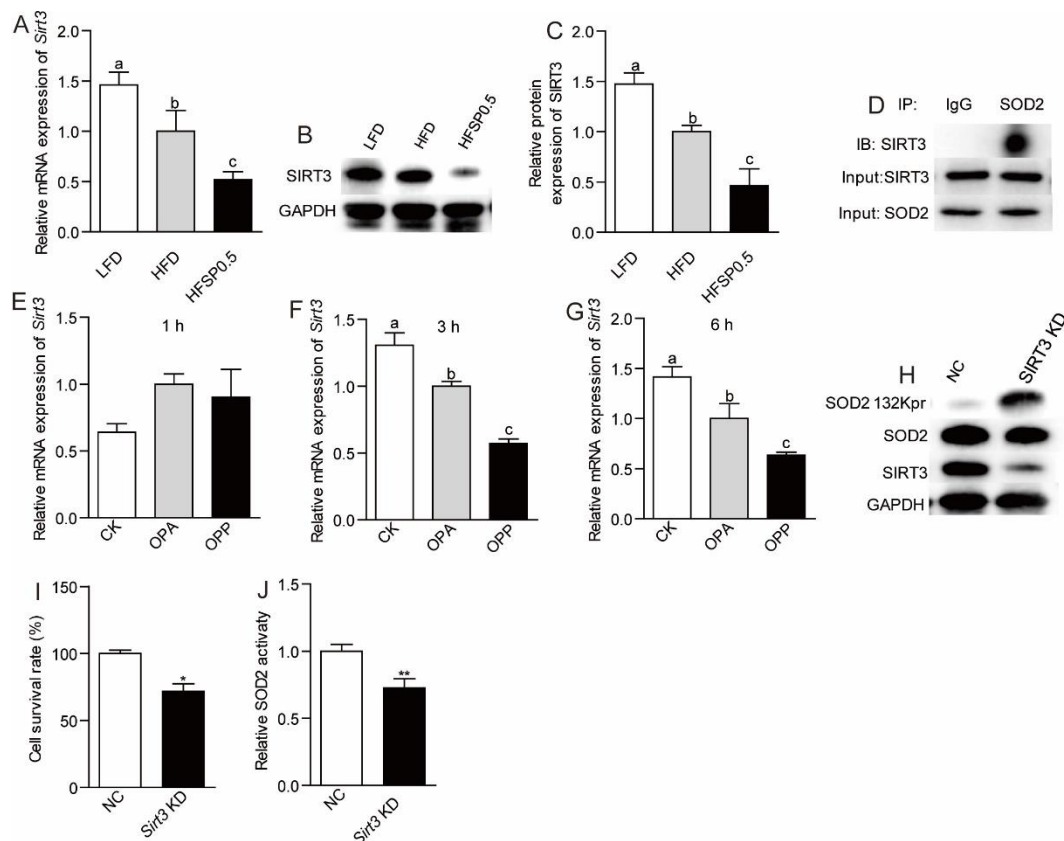
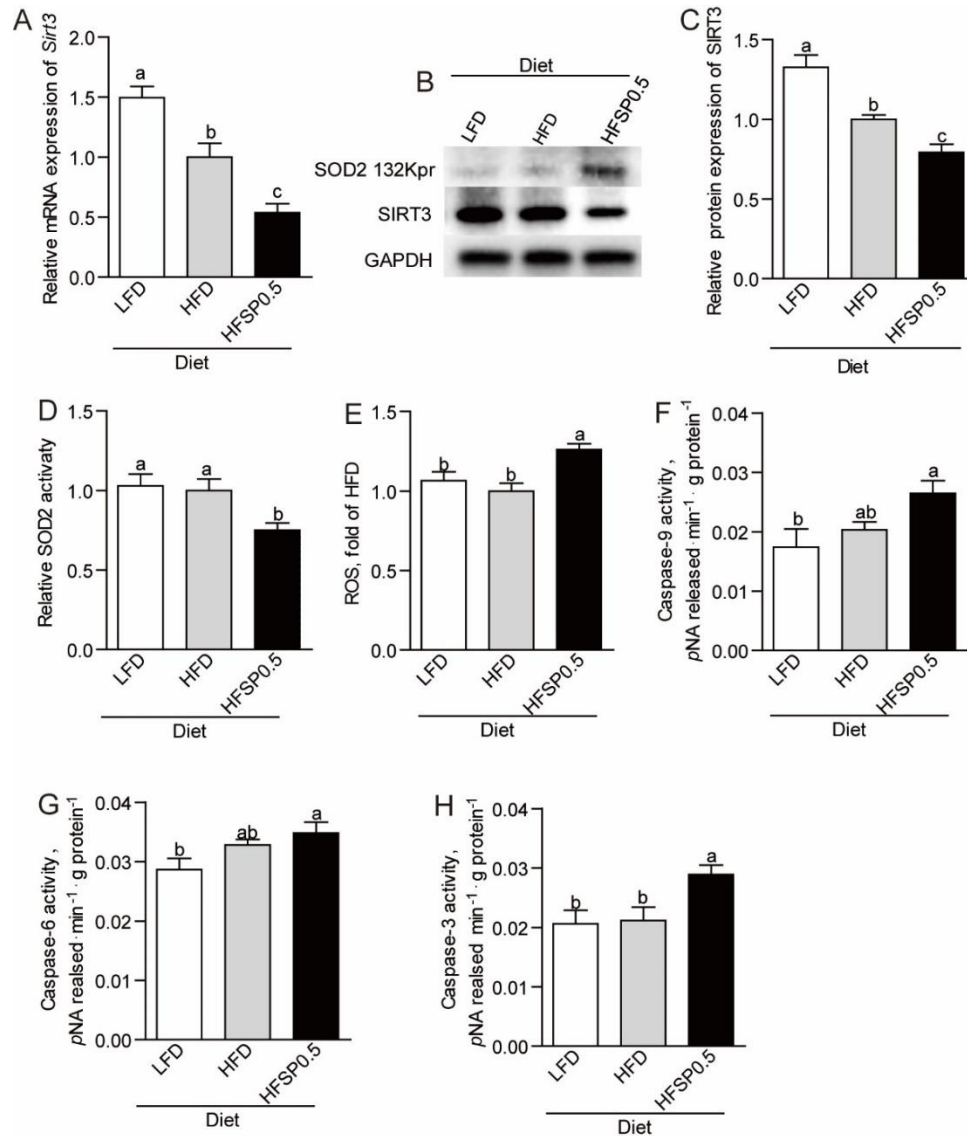


Fig. 6 Inhibition of SIRT3 promotes SOD2 propionylation. (A) Intestinal mRNA expression of *Sirt3* in zebrafish fed LFD, HFD or HFSP0.5 diet for 2 wks. (B) A representative western blotting showing expression pattern of intestinal SIRT3. (C) Quantification of intestinal SIRT3 protein level in zebrafish fed LFD, HFD or HFSP0.5 diet for 2 wks. (D) Intestinal SOD2 was immunopurified from intestine lysates with anti-SOD2 antibody, followed by western blotting with anti-SIRT3 antibody. (E-G) The mRNA expression of *Sirt3* in ZF4 cells treated with OPA or OPP in a time-dependent manner. (H) A representative western blotting showing the propionylation of SOD2 at the 132 lysine site in ZF4 cells upon *Sirt3* knockdown. (I) Cell survival rate and (J) SOD2 activity in ZF4 cells upon *Sirt3* knockdown. Values are means \pm SEMs, for A $n=6$ biological replicates; for C $n=3$ biological replicates; for E-G $n=3$ or 4 biological replicates; for I and G $n=6$ or 8 biological replicates. Means without a common letter are significantly different, $P<0.05$. * $P<0.05$, ** $P<0.01$. OPA, mixture of 150 μ M oleic acid and 50 μ M palmitic acid; OPP, mixture of 150 μ M oleic acid, 50 μ M palmitic acid and 50 mM sodium propionate.

193 **Gut microbiota contributes to ROS elevation independent of SIRT3**

194 To determine whether intestinal microbiota is required for the negative effect of
195 propionate in the context of high fat diet, we fed germ free (GF) zebrafish LFD, HFD
196 and HFSP0.5 diet and detected the expression of SIRT3. Results showed that both
197 SIRT3 mRNA level (Fig. 7A) and protein level (Fig. 7B and 7C) in GF zebrafish fed
198 HFSP0.5 diet were significantly lower than those fed HFD. These results indicated that
199 HFSP0.5 diet could directly reduce SIRT3 expression independent of gut microbiota.
200 Consistent with the compromised SIRT3 expression, the propionylation of SOD2 at
201 K132 was enhanced in GF zebrafish fed HFSP0.5 diet (Fig. 7B). Accordingly, SOD2
202 activity was reduced in GF zebrafish fed HFSP0.5 diet compared with their counterparts
203 fed HFD (Fig. 7D), and ROS was enhanced (Fig. 7E). These results indicated that
204 HFSP0.5 diet could directly induce oxidative stress via SIRT3 inhibition. Although
205 moderately induced in zebrafish fed HFSP0.5 diet compared to those fed HFD, both
206 caspase-9 and caspase-6 activity were significantly higher than in zebrafish fed LFD,
207 and caspase-3 activity was significantly induced in GF zebrafish fed HFSP0.5 diet (Fig.

208 7F-7H). These results suggest that HFSP0.5 diet activates a mitochondrial death
 209 pathway independent of gut microbiota.



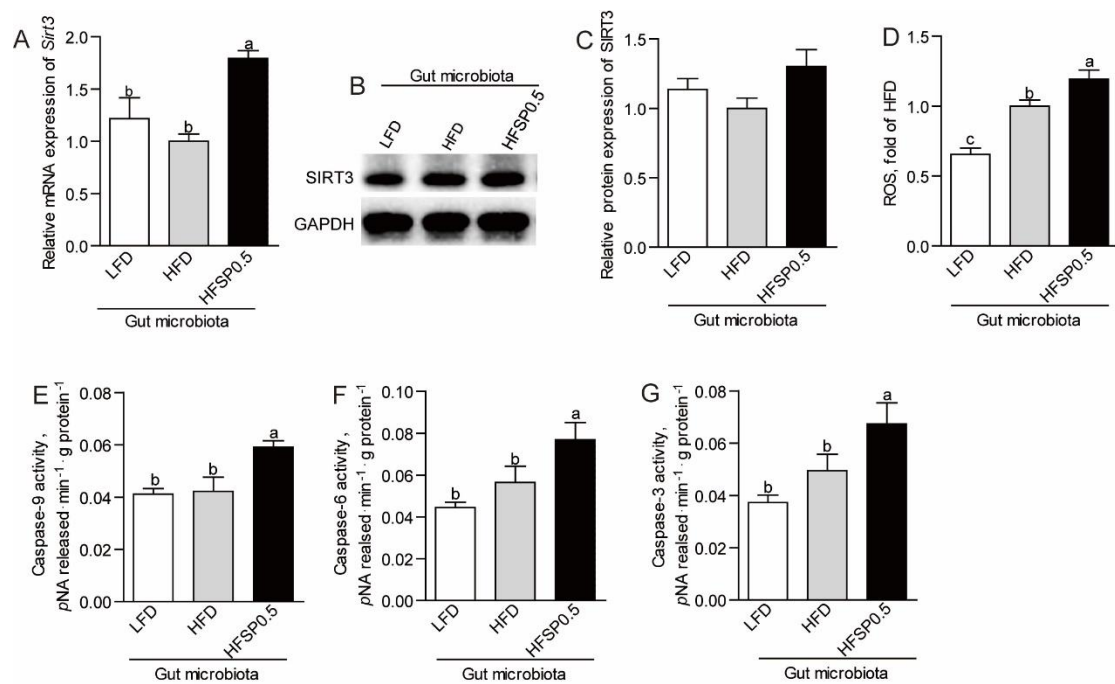
210

Fig. 7 High fat diet supplemented with 0.5% propionate directly inhibits SIRT3 expression. (A) The mRNA expression of *Sirt3* in germ-free (GF) zebrafish fed sterile LFD, HFD or HFSP0.5 diet. (B) A representative western blotting showing patterns of SIRT3 expression and SOD2 propionylation at the 132 lysine site in GF zebrafish fed sterile LFD, HFD or HFSP0.5 diet. (C) Quantification of SIRT3 protein level in GF zebrafish fed sterile LFD, HFD or HFSP0.5 diet. (D) SOD2 activity and (E) ROS level in GF zebrafish fed sterile LFD, HFD or HFSP0.5 diet. The activity of (F) caspase-9, (G) caspase-6 and (H) caspase-3 in GF zebrafish fed sterile LFD, HFD or HFSP0.5 diet. Values are means \pm SEMs, for A $n=4-6$ biological replicates; for C $n=3$ biological replicates; for D-H $n=4-8$ biological replicates. Means without a common letter are significantly different, $P<0.05$.

211

To further investigate the role of microbiota, we transferred gut microbiota from

212 zebrafish fed LFD, HFD and HFSP0.5 diet into GF zebrafish and detected the
213 expression of SIRT3. Results showed that gut microbiota from zebrafish fed HFSP0.5
214 induced moderate increase of SIRT3 expression (Fig. 8A-8C), which was different from
215 the effect of HFSP0.5 diet. These results indicated that the role of gut microbiota may
216 be independent of SIRT3. Gut microbiota from zebrafish fed HFSP0.5 diet induced
217 significant elevation of ROS (Fig. 8D). Meanwhile, the activity of caspase-9, caspase-
218 6 and caspase-3 was significantly higher in GF zebrafish colonized with HFSP0.5-
219 microbiota compared with HFD-microbiota colonized counterparts (Fig. 8E-8G). These
220 results indicated that gut microbiota induced by HFSP0.5 diet could activate the
221 mitochondrial death pathway and induce ROS independent of modulation of SIRT3
222 expression.



223

Fig. 8 Gut microbiota indirectly activate mitochondrial death pathway. (A) The mRNA expression of *Sirt3* in germ-free (GF) zebrafish transferred with gut microbiota from 1-month-old zebrafish fed LFD, HFD or HFSP0.5 diet. (B) A representative western blotting showing expression patterns of SIRT3 in GF zebrafish transferred with gut microbiota from 1-month-old zebrafish fed LFD, HFD or HFSP0.5 diet. (C) Quantification of SIRT3 protein level in GF zebrafish transferred

with gut microbiota from 1-month-old zebrafish fed LFD, HFD or HFSP0.5 diet. (D) ROS level in GF zebrafish colonized with gut microbiota from 1-month-old zebrafish fed LFD, HFD or HFSP0.5 diet. The activity of (E) caspase-9, (F) caspase-6 and (G) caspase-3 in GF zebrafish colonized with gut microbiota from 1-month-old zebrafish fed LFD, HFD or HFSP0.5 diet. Values are means \pm SEMs, for A $n=4$ or 5 biological replicates; for C-H $n=4-8$ biological replicates. Means without a common letter are significantly different, $P<0.05$.

224 **Alteration of gut microbiota is partly linked to intestinal oxidative stress induced**

225 **by propionate**

226 Considering the effect associated with the microbiota, we next investigated the
227 mechanism underlying the microbiota alteration. We observed that disturbed luminal
228 redox state was also observed in zebrafish fed HFSP0.5 diet, as evidenced by ROS
229 accumulation in gut content (Fig. 9A). Similarly, ROS level in the medium of ZF4 cells
230 treated with OPP for 24 h was significantly higher than that in cells treated by OPA (Fig.
231 9B). We analyzed the composition of gut microbiota via 16S *r*RNA gene sequencing,
232 and found that Proteobacteria and *Plesiomonas* were significantly enriched (Fig. 9C
233 and 9D, Tables 1 and 2) in zebrafish fed HFSP0.5 diet compared with those fed HFD
234 (Fig. 9C and 9D, Tables 1 and 2), though total bacterial counts were similar between
235 these two groups (Fig. 9E). The relative abundance of Firmicutes was significantly
236 lower in the HFSP0.5 group when compared with the HFD group (Fig. 9C and Table
237 1). The relative abundance of Fusobacteria and *Cetobacterium* showed the tendency of
238 decline (Fig. 9C and 9D, Tables 1 and 2).

Table 1. The predominant gut bacterial phylum in zebrafish fed on a LFD, HFD, HFSP0.5 diet for four weeks based on V3–V4 sequences.

Phylum (%)	LFD	HFD	HFSP0.5
Proteobacteria	64.06 \pm 5.94b	73.85 \pm 3.10b	89.70 \pm 1.84a
Fusobacteria	14.48 \pm 3.82a	4.65 \pm 1.87b	1.26 \pm 0.49b
Firmicutes	17.33 \pm 3.52a	15.90 \pm 2.70a	6.82 \pm 1.30b
Bacteroidetes	0.61 \pm 0.25	1.3 \pm 0.62	0.62 \pm 0.25
Actinobacteria	2.52 \pm 0.63	2.32 \pm 0.47	1.02 \pm 0.42

Values are expressed as the mean \pm SEM, n = 6. Means marked with different letters represent statistically significant results ($P < 0.05$), whereas the same letter correspond to results that show no statistically significant differences.

Table 2. The predominant gut bacterial genus in zebrafish fed on a LFD, HFD, HFSP0.5 diet for four weeks based on V3–V4 sequences.

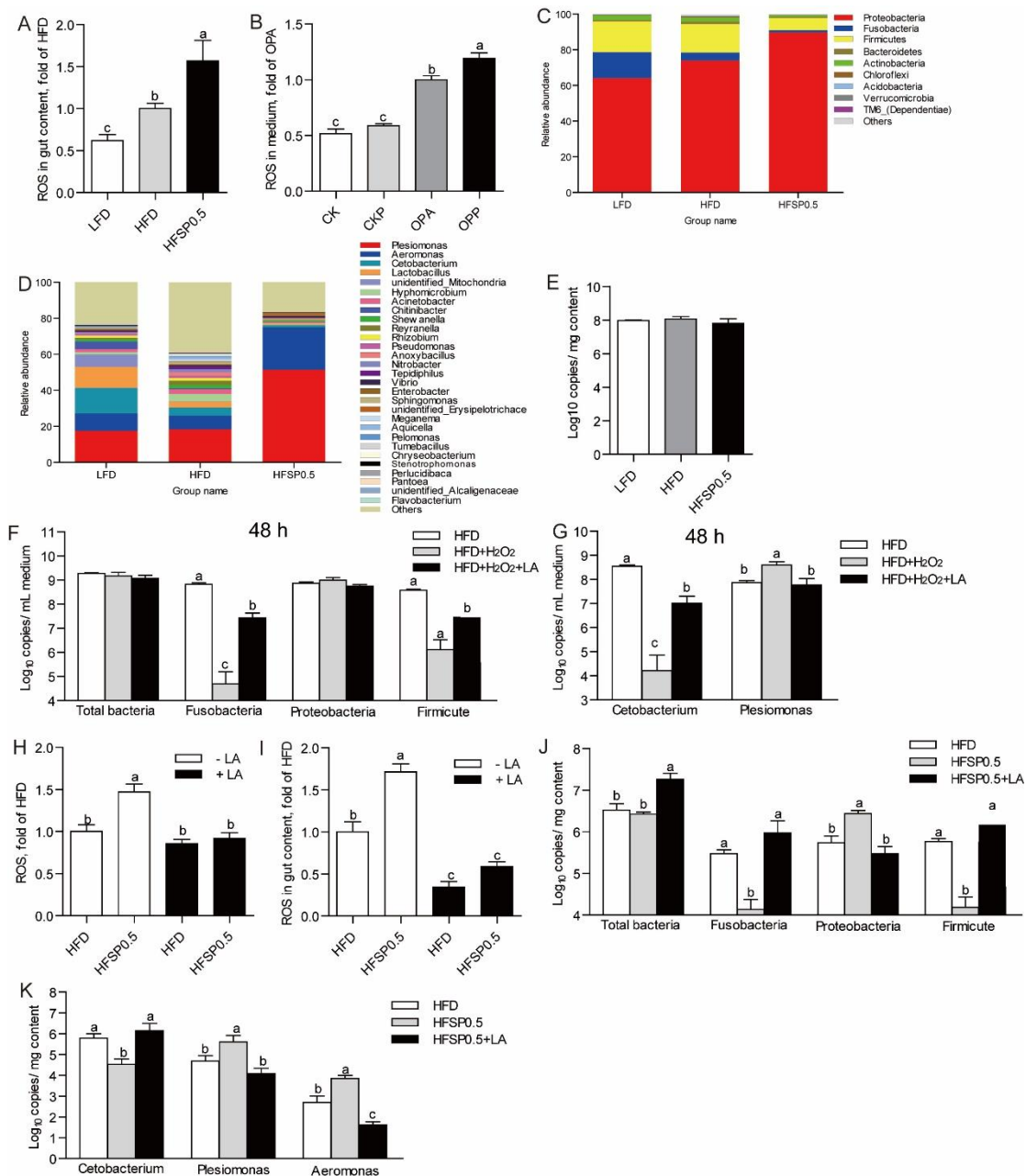
Genus (%)	LFD	HFD	HFSP0.5
Plesiomonas	17.55 \pm 6.92b	18.28 \pm 6.91b	51.41 \pm 7.24a
Aeromonas	9.59 \pm 2.37	7.60 \pm 2.46	23.51 \pm 2.60
Cetobacterium	14.27 \pm 3.78a	4.60 \pm 4.08b	1.18 \pm 4.15b
Lactobacillus	11.52 \pm 2.72a	3.24 \pm 3.27b	0.62 \pm 3.67b
Hyphomicrobium	1.26 \pm 0.29b	4.02 \pm 0.27a	0.38 \pm 0.39b
Acinetobacter	1.57 \pm 0.86ab	2.63 \pm 0.37a	0.75 \pm 0.10b
Chitinibacter	4.29 \pm 4.00	0.52 \pm 4.01	0.06 \pm 0.08

Values are expressed as the mean \pm SEM, n = 6. Means marked with different letters represent statistically significant results ($P < 0.05$), whereas the same letter correspond to results that show no statistically significant differences.

239 To determine the link between disturbed luminal redox state induced by HFSP0.5
240 diet and the composition of gut microbiota, we evaluated the effect of oxidative stress
241 on gut microbiota *in vitro* by culturing gut microbiota isolated from zebrafish fed HFD
242 in H₂O₂-supplemented GAM. Results showed that when incubated in GAM containing
243 2 mmol/L H₂O₂ for 48 h, the numbers of Fusobacteria, Firmicutes and *Cetobacterium*
244 were dramatically decreased, while Proteobacteria showed a moderate increase and the
245 number of *Plesiomonas* was significantly elevated (Fig. 9F and 9G). Meanwhile, 0.5
246 mg/mL lipoic acid (LA), a universal antioxidant, maintained the numbers of

247 Fusobacteria, Firmicutes and *Cetobacterium* similar to those cultured in GAM without
248 H₂O₂ and restricted the growth of *Plesiomonas* (Fig. 9F and 9G). These results indicated
249 that disturbed redox state may contribute to the compositional change of the intestinal
250 microbiota in zebrafish.

251 To further validate the effects of oxidative stress induced by HFSP0.5 diet on gut
252 microbiota, we performed *q*PCR to identify the numbers of Proteobacteria and
253 *Plesiomonas* in gut content collected from zebrafish fed HFSP0.5 diet with or without
254 LA. Results showed that ROS accumulation in intestine and gut content collected from
255 zebrafish fed HFSP0.5 diet was significantly alleviated by LA supplementation (Fig.
256 9H and 9I). Accordingly, the numbers of Proteobacteria and *Plesiomonas* in gut content
257 were significantly decreased by LA compared with the control (Fig. 9J and 9K).
258 Together, these results indicated that oxidative stress induced by propionate in the
259 context of HFD has the potential to switch the composition of gut microbiota by
260 elevating the abundance of Proteobacteria, which in turn further activate the
261 mitochondrial death pathway and exacerbate oxidative stress.



262

Fig. 9 Alteration of gut microbiota is partially linked to intestinal oxidative stress induced by propionate. (A) ROS level in gut content collected from zebrafish fed LFD, HFD or HFSP0.5 diet. (B) ROS level in the medium of ZF4 cells treated with OPA or OPP for 24 h. (C) The composition of gut microbiota at phylum level in 1-month-old zebrafish fed LFD, HFD or HFSP0.5 diet. (D) The composition of gut microbiota at genus level in 1-month-old zebrafish fed LFD, HFD or HFSP0.5 diet. (E) The number of total bacteria (Log₁₀ 16S *r*RNA gene copies/mg gut content) in gut content collected from 1-month-old zebrafish fed LFD, HFD or HFSP0.5 diet. (F) The number of total bacteria (Log₁₀ 16S *r*RNA gene copies/mL medium), Fusobacteria, Proteobacteria and Firmicutes after incubation in GAM with or without H₂O₂ for 48 h. (G) The numbers of *Cetobacterium* and *Plesiomonas* after incubation in GAM with or without H₂O₂ for 48 h. (H) ROS level in intestine collected from zebrafish fed HFD or HFSP0.5 diet supplemented with LA. (I) ROS level in gut content collected from zebrafish fed HFD or HFSP0.5 diet supplemented with LA. (J) The number of total bacteria (Log₁₀ 16S *r*RNA gene copies/mg gut content), Fusobacteria, Proteobacteria and

Firmicutes in gut content collected from 1-month-old zebrafish fed HFSP0.5 diet supplemented with or without LA. (K) The numbers of *Cetobacterium*, *Plesiomonas* and *Aeromonas* in gut content collected from 1-month-old zebrafish fed HFSP0.5 diet supplemented with or without LA. Values are means \pm SEMs ($n=4\sim 6$ biological replicates). Means without a common letter are significantly different, $P<0.05$.

263 **Discussion**

264 Emerging evidence suggests that propionate can be a dietary factor to ameliorate diet-
265 induced obesity (Lin et al., 2012; Lu et al., 2016; den Besten et al., 2015) and reduce
266 liver lipogenesis (Wright et al., 1990; Weitkunat et al., 2016). In this study, the anti-
267 obesity effect of propionate was also observed in zebrafish fed HFSP0.5 diet, as
268 evidenced by lower body weight gain and hepatic lipid accumulation. However,
269 oxidative stress in the intestine happened together with the anti-obesity effect of
270 propionate, as shown by elevated ROS, MDA and PC. Oxidative stress is caused by
271 ROS accumulation due to the imbalance of ROS production and removal, resulting in
272 mitochondrial dysfunction (Wei et al., 1998; Duchon, 2004; Pieczenik & Neustadt,
273 2007). SOD2 is the primary mitochondrial enzyme for ROS clearance (Spitz & Oberley,
274 1989; Zelko et al., 2002). Our study suggests that propionate impairs intestinal anti-
275 oxidant capability and SOD2 activity in the context of HFD.

276 So far, the enzyme activity of SOD2 has been shown to be regulated by an
277 ubiquitous post translational modification (PTM), acetylation (Chen et al., 2011; Assiri
278 et al., 2016; Liu et al., 2017). Among all lysine residues of SOD2 in mammals, lysine
279 sites 53, 68, 89, 122 and 130 have been shown to be acetylated (Qiu et al., 2010; Tao
280 et al., 2010; Lu et al., 2015; Zhang et al., 2016). According to the alignment of amino
281 acid sequences of SOD2 among zebrafish (EMBL no. AY195857), mice (AK002534),

282 rats (BC070913) and humans (M36693), the 132 lysine of zebrafish SOD2 is aligned
283 to the 130 lysine of mouse, rat and human SOD2 (Lin et al., 2009). Moreover, SIRT3-
284 mediated deacetylation of SOD2 (K130) can prevent ROS accumulation (Zhang et al.,
285 2016). Our results identify intestinal SOD2 lysine 132 as the propionylated lysine site
286 induced by 2-week propionate feeding under HFD. In addition, SOD2 activity could be
287 modulated by propionylation of K132, which was validated by K132Q and K132R
288 mutants that demonstrated decreased activity when lysine 132 was replaced by Gln to
289 mimic lysine propionylation, as well as decreased propionate-induced ROS level when
290 lysine 132 was replaced by Arg to mimic lysine depropionylation. Thus, lysine 132 in
291 zebrafish SOD2 is a key residue which is important for regulation of SOD2 activity.

292 Apart from SOD2, lysine propionylation was also observed in other proteins
293 (Supplementary Fig. 2) based on the global lysine propionylation analysis
294 (Supplementary Fig. 2). The first global survey of lysine propionylation has been
295 reported in Cyanobacteria (Yang et al., 2019); however, there has been no report on
296 global propionylome in animals. The bioinformatics results showed that proteins
297 involved in oxidative phosphorylation (OXPHOS) and ATP synthesis were enriched
298 among the propionylated proteins in HFSP0.5-zebrafish intestine. Besides, proteins
299 associated with the KEGG pathway of the citrate cycle (TCA cycle) were enriched for
300 lysine propionylation. Among these proteins in the TCA cycle, propionylated malate
301 dehydrogenase 2 (MDH2) and citrate synthase (CS) were found to have a complex
302 association with other mitochondrial proteins. This may indicate the potential
303 regulatory role of lysine propionylation in mitochondrial metabolism via modulating

304 functions of MDH2 and CS. SOD2 was the only propionylated antioxidant enzyme in
305 mitochondria, which was consistent with our results that blocking SOD2 propionylation
306 at K132 prevented ROS elevation in OPP-treated ZF4 cells. Nevertheless, our results
307 showed that global lysine propionylation may potentially modulate mitochondrial
308 energy metabolism, which deserves further investigation.

309 SIRT3 is a mitochondrially localized deacetylase (Michishita et al., 2005) which
310 has been reported as a central regulator of mitochondrial ROS production and is
311 required for protection from oxidative damage (Bause & Haigis, 2013). Cells lacking
312 SIRT3 are susceptible to oxidative stress (Qiu et al., 2010; Wang et al., 2014). We show
313 that propionate-induced SOD2 K132 propionylation is accompanied by depressed
314 SIRT3 expression and that SOD2 interacts with intestinal SIRT3. The sirtuin family of
315 deacetylases has been reported to have depropionylation activity. For instance, the
316 propionyl-lysine modification introduced by bacterial Gcn-5-related N-
317 acetyltransferase enzymes can be removed by bacterial and human sirtuins (Garrity et
318 al., 2007). Moreover, the absence of SIRT3 leads to a higher propionylated lysine level
319 in mouse lenses (Nahomi et al., 2020). In this study, ZF4 cells with depressed SIRT3
320 exhibited an elevated propionylation level in SOD2 132 lysine, as well as impaired
321 SOD2 activity. These results suggest a PTM mechanism involving propionylation for
322 SIRT3 modulation of SOD2 that is independent of SOD2 expression. Several studies
323 suggest that SIRT3 expression is dynamically regulated by nutrition, such as caffeine
324 and diet restriction (Zhang et al., 2015; Yu et al., 2018). Peroxisome proliferator-
325 activated receptor γ coactivator 1 α (PGC1 α) is one of few known regulators of SIRT3,

326 which can activate SIRT3 expression by binding the ERR binding element in the
327 promoter region (Kong et al., 2010). The reported transcriptional repressors including
328 poly (ADP-ribose) polymerase 1 (PARP1) and transcriptional cofactor receptor-
329 interacting protein 140 (RIP140), both of which contribute to oxidative stress and
330 mitochondrial dysfunction (Yoon & Kim, 2016; Kim et al., 2020). In this study, the
331 expression of *Pgc1 α* and *Err* in zebrafish intestine and ZF4 cells showed no significant
332 alteration in response to HFSP0.5 diet and OPP treatment (Supplementary Fig. 4),
333 suggesting that the reduction of SIRT3 expression might be mediated by its
334 transcriptional repressors.

335 Germ-free zebrafish is a convenient tool to investigate the contribution of dietary
336 factors or gut microbiota on host health and disease. Our studies demonstrate an
337 inhibitory mode to SIRT3 in the GF zebrafish model, which is independent of gut
338 microbiota. Thus, oxidative stress resulting from SOD2 propionylation is independent
339 of gut microbiota. On the other hand, gut microbiota induced by HFSP0.5 diet increased
340 ROS accumulation. Microbiota targets mitochondria to regulate interaction with the
341 host, and the mitochondrial production of ROS is often targeted by pathogenic bacteria
342 (Saint-Georges-Chaumet & Edeas, 2016). Pathogenic bacteria release various
343 pathogen-associated molecular patterns (PAMPs), including lipopolysaccharides (LPS),
344 flagellin, lipoteichoic acid, lipoprotein or other toxins, which can be recognized by the
345 pattern recognition receptor (PRR) system in the host cell surface and further induce
346 mitochondrial ROS production (Saint-Georges-Chaumet & Edeas, 2016; Emre &
347 Nubel, 2010). Therefore, the alteration in the microbiota structure might promote ROS

348 production due to differential microbe-associated molecular patterns (MAMPs)-PRR
349 signaling.

350 Gut microbiota tends to be influenced by dietary macronutrients or the
351 microenvironment in the lumen (Conlon & Bird, 2016; Hevia et al., 2015). Given that
352 the contents of fat, carbohydrates and protein were consistent between the HFD and
353 HFSP0.5 diets, the influence of dietary macronutrients can have been negligible. Thus,
354 changes of the gut microenvironment in zebrafish fed HFSP0.5 diet may have driven
355 the alteration of gut microbiota. In the present study, both intestinal oxidative stress and
356 abnormal luminal redox state occurred in zebrafish fed HFSP0.5 diet and could be
357 eliminated by LA. The reason for disturbed luminal redox state remained undiscovered,
358 but elevated ROS level in the medium of ZF4 cells treated with OPP showed that at
359 least part of ROS in lumen is released by intestinal cells. Gut microbiota in zebrafish
360 fed HFSP0.5 diet was characterized with enrichment of Proteobacteria and
361 *Plesiomonas*. Since HFSP0.5 diet-associated alteration of gut microbiota can be
362 restored by LA *in vivo*, it is reasonable to propose that luminal redox state is linked to
363 gut microbiota alteration. Besides, the quantitative results for gut microbiota cultured
364 *in vitro* showed that the numbers of Fusobacteria and Firmicutes were reduced by H₂O₂,
365 whereas the Proteobacteria population showed a modest increase. This suggested that
366 Proteobacteria are more resilient to oxidative stress than Fusobacteria and Firmicutes,
367 which may explain the enrichment of Proteobacteria in a disturbed redox state. Our
368 results indicated that gut microbiota acted both as a responder and as a secondary
369 inducer of the intestinal oxidative stress, while the original cause was attributed to

370 propionate and HFD.

371 One intriguing finding in our work is that propionate only induces oxidative
372 damage to the intestine under a high fat background. Considering that propionate-
373 induced oxidative damage is mediated by the modulation of SOD2 lysine 132
374 propionylation, SIRT3 and propionyl-CoA metabolism are important to illuminate the
375 effect of dietary fat on propionate toxicity. SIRT3 expression can be depressed by
376 nutritional stress, such as alcohol and HFD (Ma et al., 2019; Palacios et al., 2009).
377 Mitochondrial protein propionylation increases in response to chronic ethanol ingestion
378 in mice, similar to mitochondrial protein acetylation (Fritz et al., 2013). In this study,
379 we show that intestinal SIRT3 expression in zebrafish fed HFD is lower than in
380 zebrafish fed LFD. Propionyl-CoA carboxylase (PCC) is the essential enzyme
381 catalyzing the carboxylation of propionyl-CoA to methylmalonyl-CoA, ultimately
382 contributes to the succinyl-CoA pool and enters the TCA cycle (Wongkittichote &
383 Chapman, 2017; Xu et al., 2018). Our results show that HFD inhibits PCC expression,
384 which may disrupt the conversion of propionyl-CoA to succinyl-CoA. Deficiency of
385 PCC leads to accumulation of propionyl-CoA (Wongkittichote & Chapman, 2017). The
386 results presented above suggest that the capability of intestine for depropionylation and
387 metabolism of propionyl-CoA are weakened by HFD. Although the contribution of
388 HFD to SOD2 propionylation remains unclear, a high level of dietary fat promotes the
389 potential adverse effects of propionate.

390 In clinical research, individuals with ASD are four times as likely to experience
391 gastrointestinal (GI) symptoms as healthy controls (McElhanon et al., 2014). An

392 important factor in the pathogenesis of ASD is gut microbiota, such as *Clostridium* spp.,
393 and its metabolites, especially propionate (Wang et al., 2014). There is some evidence
394 that gut microbiota (Strati et al., 2017; Finegold et al., 2010), increased intestinal
395 inflammation (Nina & David, 2017) and mitochondrial dysfunction (Frye et al., 2015)
396 may play a role in ASD-associated GI symptoms, but the pathogenesis has not been
397 well defined. The results in our study suggest that propionate-induced propionylation
398 of antioxidant proteins and the resultant intestinal oxidative stress may contribute to
399 GI-related comorbidities in ASD. In another metabolic disorder known as propionic
400 acidemia (PA), the accumulation of propionyl CoA results in mitochondrial dysfunction
401 and oxidative stress (de Keyzer et al., 2009; Gallego-Villar et al., 2013; Gallego-Villar
402 et al., 2016). Meanwhile, fibroblasts from patients with PA show increased protein
403 propionylation, which leads to impaired mitochondrial respiration (Pougovkina, 2016).
404 Although studies suggest the role of protein propionylation and oxidative stress in the
405 pathological mechanism of PA, how protein propionylation manipulates oxidative
406 stress was unmentioned and the identification of propionylated proteins has been
407 lacking. Our results identified propionylated SOD2 as a direct cause of oxidative stress,
408 implying that a similar mechanism may apply to PA pathogenesis.

409 The results presented above suggest that propionate in the context of high fat diet
410 induces SOD2 propionylation at the 132 lysine site, which compromises the superoxide
411 scavenging function of SOD2 and induces oxidative stress in zebrafish intestine. SIRT3
412 can directly interact with SOD2 and plays an important role in regulating SOD2 activity
413 via modulating propionylation at K132, and the enhanced SOD2 propionylation in

414 zebrafish fed high fat plus propionate diet was attributed to reduced SIRT3 expression.
415 Although the connection between SIRT3-mediated deacetylation and SOD2 activation
416 has been well demonstrated, this is the first identification of the link between SIRT3-
417 mediated depropionylation and SOD2 activity. Furthermore, our results indicated that
418 the intestinal microbiota associated with high fat plus propionate diet also induces
419 oxidative stress in zebrafish intestine, but in a SIRT3-independent manner, while the
420 oxidative stress contributes to the shaping of the microbiota. Considering propionate is
421 a widely used food and feed preservative, our findings have important implications for
422 the safety of propionate as a food additive, especially in the context of high fat diet.

423 **Materials and Methods**

424 **Fish husbandry**

425 All of the experimental and animal care procedures were approved by the Feed
426 Research Institute of the Chinese Academy of Agricultural Sciences Animal Care
427 Committee under the auspices of the China Council for Animal Care (Assurance No.
428 2016-AF-FRI-CAAS-001). One-month-old zebrafish were maintained at the zebrafish
429 facility of the Feed Research Institute of the Chinese Academy of Agricultural Sciences
430 (Beijing, China) and fed with the experimental diets (Supplementary Table 1) twice a
431 day (9:00, 17:00) to apparent satiation each time for 2 weeks. During the feeding period,
432 the rearing temperature was 25-28 °C, the dissolved oxygen was > 6.0 mg/L, the pH
433 was 7.0 - 7.2, the nitrogen content was < 0.50 mg · L⁻¹, and the nitrogen content (as
434 NO₂) was < 0.02 mg · L⁻¹. All fish were anesthetized with tricaine methanesulfonate
435 (MS222).

436 **Examination of intestinal histopathology**

437 The intestines of zebrafish were rinsed with sterilized PBS, fixed in 4% formalin
438 solution, and embedded in paraffin. For histological analysis, the liver sections prepared
439 from the paraffin blocks were stained with hematoxylin and eosin (H&E). Images were
440 obtained under a microscope (Carl Zeiss) at a 200× magnification.

441 **Intraperitoneal injection of 4-Hydroxy-TEMPO**

442 After 2-wk feeding trial, ten zebrafish from LFD, HFD and HFSP0.5 groups were
443 respectively divided into two groups: 1) control zebrafish injected intraperitoneally (i.p.)
444 with saline (0.9% NaCl); 2) zebrafish treated i.p. with Tempol dissolved in saline (10
445 mg/kg b.w.) every other day. Intestines were collected at the sixth day for H&E staining.

446 **Detection of caspase activity**

447 The activities of caspase-3, caspase-6 and caspase-9 were determined using an assay
448 kit (Beyotime Biotechnology, Shanghai, China) according to the manufacturer's
449 instructions. The optical density of the reaction product was examined at 405 nm. The
450 enzyme activity units were expressed as the rate of *p*-nitroaniline (*p*NA) released from
451 the substrate per gram protein ($\mu\text{mol } p\text{NA released} \cdot \text{min}^{-1} \cdot \text{g protein}^{-1}$).

452 **Mitochondria isolation and mitochondrial reactive oxygen species determination**

453 Intestine was used to perform mitochondria isolation by using a tissue mitochondria
454 isolation kit (Beyotime Biotechnology, Shanghai, China) according to the
455 manufacturer's instructions. We adjusted mitochondria to the same level according to
456 mitochondria protein level. Mitochondria isolated were then subjected to reactive
457 oxygen species (ROS) assay using fluorometric intracellular ROS kit (Sigma, USA).

458 The fluorescence was acquired with excitation and emission wavelengths of 490 nm
459 and 520 nm, respectively. ROS level was expressed as the fold of the HFD group.

460 **Detection of oxidative parameters**

461 Lipid peroxidation was determined by the reaction of malondialdehyde (MDA) with
462 thiobarbituric acid to form a colorimetric product by using a lipid peroxidation assay
463 kit according to the manufacturer's instructions (Sigma, USA). The optical density of
464 the reaction product was examined at 532 nm. Lipid peroxidation was expressed as
465 MDA content per 100 milligram tissue ($\text{nmol} \cdot 100 \text{ mg tissue}^{-1}$). Oxidation of proteins
466 was determined by the formation of stable dinitrophenyl hydrazine adducts derived
467 from protein carbonyl (PC) groups with 2, 4-dinitrophenylhydrazine using protein
468 carbonyl content assay kit according to the manufacturer's instructions (Sigma, USA).
469 The optical density of the adduct was examined at 375 nm. Oxidation of proteins was
470 expressed as PC content per milligram protein ($\text{nmol} \cdot \text{mg protein}^{-1}$).

471 **Evaluation of total antioxidant capacity**

472 Total antioxidant capacity (T-AOC) was measured by the production of blue Fe^{2+} -TPTZ
473 resulting from the reduction of Fe^{3+} TPTZ complex in acidic conditions. The optical
474 density was measured at 593 nm. T-AOC was defined as the production of FeSO_4 per
475 gram protein ($\text{mmol FeSO}_4 \cdot \text{g protein}^{-1}$).

476 **Evaluation of antioxidant enzyme activity**

477 The activity of SOD2, glutathione peroxidase (GPx) and catalase (CAT) were detected
478 using a CuZn/Mn-SOD activity kit, a cellular GPx assay kit and a catalase assay kit
479 (Beyotime Biotechnology, Shanghai, China), respectively, according to the

480 manufacturer's instructions. SOD2 activity was measured as the inhibition of water
481 soluble tetrazol salt (WST-8) reduction in a xanthine-xanthine oxidase system. The
482 SOD2 activity in intestine was expressed as $U \cdot mg \text{ protein}^{-1}$. Relative SOD2 activity
483 in ZF4 cell and zebrafish larva was expressed as fold of indicated group. The activity
484 of GPx was expressed as $mU \cdot mg \text{ protein}^{-1}$. The activity of CAT was expressed as
485 $U \cdot mg \text{ protein}^{-1}$.

486 **Gut microbiota analysis**

487 The 16s V3 - V4 region was amplified using the primers U341F (5'-
488 CGGCAACGAGCGCAACCC-3') and U806 (5'-CCATTGTAGCACGTGTGTAGCC-
489 3'). The 16S ribosomal RNA gene sequencing was performed by Novogene
490 Bioinformatics Technology Co. Ltd (Beijing, China) using the Illumina HiSeq platform.
491 Then the raw pair-end readings were subjected to a quality-control procedure using the
492 UPARSE-operational taxonomic unit (OTU) algorithm. The qualified reads were
493 clustered to generate OTUs at the 97% similarity level using the USEARCH sequence
494 analysis tool. A representative sequence of each OTU was assigned to a taxonomic level
495 in the Ribosomal Database Project (RDP) database using the RDP classifier. Principal
496 component analysis and heat-map analysis were performed by using R 3.1.0.

497 **GF-zebrafish generation and treatment**

498 GF-zebrafish were derived from normal zebrafish and reared following established
499 protocols (Rawls et al., 2006). We formulated microparticulate diets, namely LFD, HFD,
500 and HFSP0.5 diets, for zebrafish larvae (Supplementary Table 2). Before feeding, the
501 microparticulate diets were sterilized by irradiation with 20 kGy gamma ray in an

502 atomic energy center (Institute of Food Science and Technology, Chinese Academy of
503 Agricultural Sciences, Beijing, China). Zebrafish larvae hatched from their chorions at
504 3 days postfertilization (dpf). Each group had six bottles with 20 fish per bottle. At 5
505 dpf, the yolk was largely absorbed and the GF-zebrafish started feeding. At 11 dpf,
506 whole fish were collected for analysis of caspase activity, SOD2 activity, *q*PCR or
507 western blotting.

508 **Cell culture**

509 The ZF4 cell line was purchased from American Type Culture Collection (Manassas,
510 VA, USA), and cultured according to established protocols (Driever & Rangini, 1993).
511 The media were obtained from Corning Inc. (New York, NY, USA). Penicillin-
512 Streptomycin solution and bovine insulin were purchased from Sigma (St. Louis, MO,
513 USA). Fetal bovine serum was purchased from Corning Inc. (New York, NY, USA).

514 **Cell viability analysis**

515 ZF4 cell was first seeded on 96-well plates and incubated for 24 h to sub-confluence.
516 Then ZF4 cell was exposed to fresh medium added with a mixture of 150 μ M OA and
517 50 μ M PA (OPA), and a mixture of 150 μ M OA, 50 μ M PA and 50 mM propionate
518 (OPP). At the end of the exposure period, fresh medium with 10% AlarmaBlue cell
519 viability reagent (Invitrogen, Grand Island, NY, USA) was added. After a 1-h
520 incubation, fluorescence was measured with the SynergyMX Multi-Functional
521 Detector (Biotek, Winooski, VT, USA) at excitation and emission wavelengths of 485
522 nm and 595 nm, respectively. The ratio of cell viability was calculated using the
523 fluorescence readings of the control and treatments.

524 **Cell apoptosis analysis**

525 Cell apoptosis detection was performed with Annexin V-fluorescein isothiocyanate
526 (FITC) kits (Sigma). After exposure to OPA or OPP for 24 h, the cells were collected
527 and incubated with Annexin V-FITC and propidium iodide in binding buffer for 10 min
528 in darkness at room temperature. The analysis was conducted by the Guava easyCyte
529 Flow Cytometer (Merck Millipore, Stafford, VA, USA).

530 **Gene silencing with siRNA**

531 Scrambled siRNA (negative control), *Sod2* and *Sirt3* siRNA (Supplementary Table 3)
532 were synthesized by GenePharma Co. Ltd. (Shanghai, China). Cells were first seeded
533 on 6-well plates (Corning) and incubated for 24 h to sub-confluence. Then the cells
534 were transfected with the appropriate siRNAs using Lipofectamine RNAiMAX
535 Transfection Reagent (Invitrogen). Efficiency of the siRNA was determined by qPCR.

536 **Effects of oxidative stress on gut microbiota *in vitro***

537 Fresh gut content samples pooled from five zebrafish were put on ice and diluted in 5
538 mL sterile, ice-cold PBS. Within 30 min of sample collection, bacteria were cultured
539 on Gifu anaerobic medium (GAM); GAM supplemented with 2 mmol/L H₂O₂
540 (GAM+H₂O₂); GAM+H₂O₂+LA, GAM supplemented with 2 mmol/L H₂O₂ and 0.05 %
541 LA. After an incubation period of 48 h at 28 °C, the number of total bacteria or a specific
542 phylotype was quantified by qPCR according to Zhang et al (73 Zhang et al., 2019).
543 Primer sets for universal bacteria or specific bacterial groups targeting the 16S rRNA
544 gene are listed in Supplementary Table 4. For the gut microbiota cultured *in vitro*,
545 results were expressed as Log₁₀ copy numbers of bacterial 16S rDNA per mL medium

546 (Log₁₀ copies/mL medium).

547 **Plasmid construction and transfection**

548 The SOD2 was cloned into *pCDNA3.1*. Point (Site) mutations of SOD2 were generated
549 by QuikChange Site-Directed Mutagenesis kit (Stratagene). Both WT SOD2 and SOD2
550 mutant plasmids were transfected into ZF4 cells using Lipofectamine 3000 Transfection
551 Reagent (Invitrogen).

552 **Western blotting**

553 Zebrafish intestine or larval zebrafish were homogenized in ice-cold HBSS buffer
554 mixed with 1 mM PMSF and phosphatase inhibitors. Equivalent amounts of total
555 protein were loaded into a 12% SDS-PAGE for electrophoresis and then transferred into
556 a PVDF membrane (Millipore, USA). After blocking nonspecific binding with 5%
557 skimmed milk in TBST, the PVDF membrane was incubated with primary antibodies,
558 i.e., antibodies against GAPDH (Sigma, SAB2708126, 1:2000), SOD2 (Genetex,
559 GTX124294, 1:1000), SIRT3 (Sigma, AV32388, 1:1000) and customized SOD2
560 k132pro (Jingjie, 1:500). The blots were developed using HRP-conjugated secondary
561 antibodies (GE Health, 1:3000) and the ECL-plus system.

562 **Total RNA extraction, reverse transcription, and qPCR**

563 Total RNA was isolated using Trizol reagent and then reverse transcribed to cDNA. The
564 qPCR was performed using SYBR®Green Supermix according to the manufacturer's
565 instructions (Tiangen, Beijing, China). The results were stored, managed, and analyzed
566 via LightCycler 480 software (Roche, Basel, Switzerland). The qPCR primers used are
567 listed in Supplementary Table 4.

568 **Data analysis**

569 All of the statistical analyses were conducted using GraphPad Prism 5 software
570 (GraphPad Software Inc., San Diego, CA, USA). Results are expressed as the means \pm
571 standard errors of the means (SEMs). Comparisons between two groups were analyzed
572 using the Student's *t*-test, and comparisons between multiple groups were analyzed
573 using one-way ANOVA followed by a Duncan's test. The statistical significance was
574 set at $P < 0.05$.

575 **References**

- 576 1. Koh, A., De Vadder, F., Kovatcheva-Datchary, P., & Backhed, F. (2016). From
577 Dietary Fiber to Host Physiology: Short-Chain Fatty Acids as Key Bacterial
578 Metabolites. *Cell*, 165(6), 1332-1345. <https://doi.org/10.1016/j.cell.2016.05.041>
- 579 2. Rose, M. D. . (2013). Efsa panel on food additives and nutrient sources added to
580 food (ans). *EFSA Journal*, 11(6), 3234.
- 581 3. Ng, W. K., & Koh, C. B. (2017). The utilization and mode of action of organic
582 acids in the feeds of cultured aquatic animals. *Reviews in Aquaculture*, 9(4), 342-
583 368. <https://doi.org/10.1111/raq.12141>
- 584 4. Matsuishi, T., Stumpf, D. A., Seliem, M., Eguren, L. A., & Chrislip, K. (1991).
585 Propionate mitochondrial toxicity in liver and skeletal muscle: acyl CoA levels.
586 *Biochem Med Metab Biol*, 45(2), 244-253. [https://doi.org/10.1016/0885-
587 4505\(91\)90027-i](https://doi.org/10.1016/0885-4505(91)90027-i)
- 588 5. Pougovkina, O.A. (2016). Functional interplay between protein acylation and
589 cellular metabolism in metabolic disorders [D]. *AMC-UvA*, 1-159.
- 590 6. Stumpf, D. A., McAfee, J., Parks, J. K., & Eguren, L. (1980). Propionate inhibition
591 of succinate:CoA ligase (GDP) and the citric acid cycle in mitochondria. *Pediatr*
592 *Res*, 14(10), 1127-1131. <https://doi.org/10.1203/00006450-198010000-00008>
- 593 7. Frye, R. E., Rose, S., Slattery, J., & MacFabe, D. F. (2015). Gastrointestinal

- 594 dysfunction in autism spectrum disorder: the role of the mitochondria and the
595 enteric microbiome. *Microb Ecol Health Dis*, 26, 27458.
596 <https://doi.org/10.3402/mehd.v26.27458>
- 597 8. Schonfeld, P., & Wojtczak, L. (2016). Short- and medium-chain fatty acids in
598 energy metabolism: the cellular perspective. *J Lipid Res*, 57(6), 943-954.
599 <https://doi.org/10.1194/jlr.R067629>
- 600 9. Flavin, M., & Ochoa, S. (1957). Metabolism of propionic acid in animal tissues. I.
601 Enzymatic conversion of propionate to succinate. *J Biol Chem*, 229(2), 965-979.
602 <http://www.ncbi.nlm.nih.gov/pubmed/13502357>
- 603 10. Chen, Y., Sprung, R., Tang, Y., Ball, H., Sangras, B., Kim, S. C., Falck, J. R., Peng,
604 J., Gu, W., & Zhao, Y. (2007). Lysine propionylation and butyrylation are novel
605 post-translational modifications in histones. *Mol Cell Proteomics*, 6(5), 812-819.
606 <https://doi.org/10.1074/mcp.M700021-MCP200>
- 607 11. Cheng, Z., Tang, Y., Chen, Y., Kim, S., Liu, H., Li, S. S., Gu, W., & Zhao, Y.
608 (2009). Molecular characterization of propionyllysines in non-histone proteins. *Mol*
609 *Cell Proteomics*, 8(1), 45-52. <https://doi.org/10.1074/mcp.M800224-MCP200>
- 610 12. Liu, B., Lin, Y. H., Darwanto, A., Song, X. H., Xu, G. L., & Zhang, K. L. (2009).
611 Identification and Characterization of Propionylation at Histone H3 Lysine 23 in
612 Mammalian Cells. *Journal of Biological Chemistry*, 284(47), 32288-32295.
613 <https://doi.org/10.1074/jbc.M109.045856>
- 614 13. Zhang, K., Chen, Y., Mang, Z. H., & Zhao, Y. M. (2009). Identification and
615 Verification of Lysine Propionylation and Butyrylation in Yeast Core Histones
616 Using PTMap Software. *Journal of Proteome Research*, 8(2), 900-906.
617 <https://doi.org/10.1021/pr8005155>
- 618 14. Kebede, A. F., Nieborak, A., Shahidian, L. Z., Le Gras, S., Richter, F., Gomez, D.
619 A., Baltissen, M. P., Meszaros, G., Magliarelli, H. D., Taudt, A., Margueron, R.,
620 Colome-Tatche, M., Ricci, R., Daujat, S., Vermeulen, M., Mittler, G., & Schneider,
621 R. (2017). Histone propionylation is a mark of active chromatin. *Nature Structural*
622 *& Molecular Biology*, 24(12), 1048-+. <https://doi.org/10.1038/nsmb.3490>
- 623 15. Bhatti, J. S., Bhatti, G. K., & Reddy, P. H. (2017). Mitochondrial dysfunction and

- 624 oxidative stress in metabolic disorders - A step towards mitochondria based
625 therapeutic strategies. *Biochimica Et Biophysica Acta-Molecular Basis of Disease*,
626 *1863*(5), 1066-1077. <https://doi.org/10.1016/j.bbadis.2016.11.010>
- 627 16. Wei, Y. H., Lu, C. Y., Lee, H. C., Pang, C. Y., & Ma, Y. S. (1998). Oxidative
628 damage and mutation to mitochondrial DNA and age-dependent decline of
629 mitochondrial respiratory function. *Towards Prolongation of the Healthy Life Span*,
630 *854*, 155-170. [https://doi.org/DOI 10.1111/j.1749-6632.1998.tb09899.x](https://doi.org/DOI%2010.1111/j.1749-6632.1998.tb09899.x)
- 631 17. Duchen, M. R. (2004). Mitochondria in health and disease: perspectives on a new
632 mitochondrial biology. *Mol Aspects Med*, *25*(4), 365-451.
633 <https://doi.org/10.1016/j.mam.2004.03.001>
- 634 18. Pieczenik, S. R., & Neustadt, J. (2007). Mitochondrial dysfunction and molecular
635 pathways of disease. *Experimental and Molecular Pathology*, *83*(1), 84-92.
636 <https://doi.org/10.1016/j.yexmp.2006.09.008>
- 637 19. Palucka, T. (2007). Toying with a ridiculous material. *Mrs Bulletin*, *32*(3), 283-283.
638 [https://doi.org/Doi 10.1557/Mrs2007.31](https://doi.org/Doi%2010.1557/Mrs2007.31)
- 639 20. Novak, E. A., & Mollen, K. P. (2015). Mitochondrial dysfunction in inflammatory
640 bowel disease. *Front Cell Dev Biol*, *3*, 62. <https://doi.org/10.3389/fcell.2015.00062>
- 641 21. Rafi SS. (1998). Studies on the pathogenesis of NSAID-induced damage to the
642 gastrointestinal tract with special reference to the mitochondria. ETH:326317.
- 643 22. Somasundaram, S., Rafi, S., Hayllar, J., Sigthorsson, G., Jacob, M., Price, A. B.,
644 Macpherson, A., Mahmood, T., Scott, D., Wrigglesworth, J. M., & Bjarnason, I.
645 (1997). Mitochondrial damage: a possible mechanism of the "topical" phase of
646 NSAID induced injury to the rat intestine. *Gut*, *41*(3), 344-353.
647 <https://doi.org/10.1136/gut.41.3.344>
- 648 23. Kyle S. Saitta. (2014). Mechanisms of NSAID-Induced Small Intestinal Injury:
649 Role of Bacterial Beta-Glucuronidase, the Microbiome, and Mitochondria.
650 *Microbiology & Immunology*, *28*, 975-86.
- 651 24. Bhattacharyya, S., Dudeja, P. K., & Tobacman, J. K. (2009). ROS, Hsp27, and
652 IKKbeta mediate dextran sodium sulfate (DSS) activation of IkappaBa, NFkappaB,

- 653 and IL-8. *Inflamm Bowel Dis*, 15(5), 673-683. <https://doi.org/10.1002/ibd.20821>
- 654 25. Bhattacharyya, A., Chattopadhyay, R., Mitra, S., & Crowe, S. E. (2014). Oxidative
655 Stress: An Essential Factor in the Pathogenesis of Gastrointestinal Mucosal
656 Diseases. *Physiological Reviews*, 94(2), 329-354.
657 <https://doi.org/10.1152/physrev.00040.2012>
- 658 26. Circu, M. L., & Aw, T. Y. (2012). Intestinal redox biology and oxidative stress.
659 *Seminars in Cell & Developmental Biology*, 23(7), 729-737.
660 <https://doi.org/10.1016/j.semcdb.2012.03.014>
- 661 27. Bheda, P., Wang, J. T., Escalante-Semerena, J. C., & Wolberger, C. (2011).
662 Structure of Sir2Tm bound to a propionylated peptide. *Protein Science*, 20(1), 131-
663 139. <https://doi.org/10.1002/pro.544>
- 664 28. Lin, H. V., Frassetto, A., Kowalik, E. J., Nawrocki, A. R., Lu, M. F. M., Kosinski,
665 J. R., Hubert, J. A., Szeto, D., Yao, X. R., Forrest, G., & Marsh, D. J. (2012).
666 Butyrate and Propionate Protect against Diet-Induced Obesity and Regulate Gut
667 Hormones via Free Fatty Acid Receptor 3-Independent Mechanisms. *Plos One*, 7(4).
668 <https://doi.org/ARTN e35240 10.1371/journal.pone.0035240>
- 669 29. Lu, Y. Y., Fan, C. N., Li, P., Lu, Y. F., Chang, X. L., & Qi, K. M. (2016). Short
670 Chain Fatty Acids Prevent High-fat-diet-induced Obesity in Mice by Regulating G
671 Protein-coupled Receptors and Gut Microbiota. *Scientific Reports*, 6.
672 <https://doi.org/Artn 37589 10.1038/Srep37589>
- 673 30. den Besten, G., Bleeker, A., Gerding, A., van Eunen, K., Havinga, R., van Dijk, T.
674 H., Oosterveer, M. H., Jonker, J. W., Groen, A. K., Reijngoud, D. J., & Bakker, B.
675 M. (2015). Short-Chain Fatty Acids Protect Against High-Fat Diet-Induced Obesity
676 via a PPAR-Dependent Switch From Lipogenesis to Fat Oxidation. *Diabetes*, 64(7),
677 2398-2408. <https://doi.org/10.2337/db14-1213>
- 678 31. Wright, R. S., Anderson, J. W., & Bridges, S. R. (1990). Propionate inhibits
679 hepatocyte lipid synthesis. *Proc Soc Exp Biol Med*, 195(1), 26-29.
680 <https://doi.org/10.3181/00379727-195-43113>
- 681 32. Weitkunat, K., Schumann, S., Nickel, D., Kappo, K. A., Petzke, K. J., Kipp, A. P.,
682 Blaut, M., & Klaus, S. (2016). Importance of propionate for the repression of

- 683 hepatic lipogenesis and improvement of insulin sensitivity in high-fat diet-induced
684 obesity. *Mol Nutr Food Res*, 60(12), 2611-2621.
685 <https://doi.org/10.1002/mnfr.201600305>
- 686 33. Spitz, D. R., & Oberley, L. W. (1989). An assay for superoxide dismutase activity
687 in mammalian tissue homogenates. *Anal Biochem*, 179(1), 8-18.
688 [https://doi.org/10.1016/0003-2697\(89\)90192-9](https://doi.org/10.1016/0003-2697(89)90192-9)
- 689 34. Zelko, I. N., Mariani, T. J., & Folz, R. J. (2002). Superoxide dismutase multigene
690 family: a comparison of the CuZn-SOD (SOD1), Mn-SOD (SOD2), and EC-SOD
691 (SOD3) gene structures, evolution, and expression. *Free Radic Biol Med*, 33(3),
692 337-349. [https://doi.org/10.1016/s0891-5849\(02\)00905-x](https://doi.org/10.1016/s0891-5849(02)00905-x)
- 693 35. Chen, Y. H., Zhang, J. Y., Lin, Y., Lei, Q. Y., Guan, K. L., Zhao, S. M., & Xiong,
694 Y. (2011). Tumour suppressor SIRT3 deacetylates and activates manganese
695 superoxide dismutase to scavenge ROS. *Embo Reports*, 12(6), 534-541.
696 <https://doi.org/10.1038/embor.2011.65>
- 697 36. Assiri, M., Harris, P. S., Ali, H., Liang, Y. L., Shearn, C. T., Roede, J. R., Backos,
698 D. S., & Fritz, K. S. (2016). Chronic Ethanol Consumption Alters SOD2 Dynamics
699 through Lysine Acetylation. *Free Radical Biology and Medicine*, 100, S98-S99.
700 <https://doi.org/10.1016/j.freeradbiomed.2016.10.247>
- 701 37. Liu, X. H., Zhang, L., Wang, P., Li, X. Y., Qiu, D. H., Li, L., Zhang, J. Q., Hou, X.
702 J., Han, L. S., Ge, J., Li, M., Gu, L., & Wang, Q. (2017). Sirt3-dependent
703 deacetylation of SOD2 plays a protective role against oxidative stress in oocytes
704 from diabetic mice. *Cell Cycle*, 16(13), 1302-1308.
705 <https://doi.org/10.1080/15384101.2017.1320004>
- 706 38. Qiu, X. L., Brown, K., Hirschey, M. D., Verdin, E., & Chen, D. (2010). Calorie
707 Restriction Reduces Oxidative Stress by SIRT3-Mediated SOD2 Activation. *Cell*
708 *Metabolism*, 12(6), 662-667. <https://doi.org/10.1016/j.cmet.2010.11.015>
- 709 39. Tao, R. D., Coleman, M. C., Pennington, J. D., Ozden, O., Park, S. H., Jiang, H. Y.,
710 Kim, H. S., Flynn, C. R., Hill, S., McDonald, W. H., Olivier, A. K., Spitz, D. R., &
711 Gius, D. (2010). Sirt3-Mediated Deacetylation of Evolutionarily Conserved Lysine
712 122 Regulates MnSOD Activity in Response to Stress. *Molecular Cell*, 40(6), 893-

- 713 904. <https://doi.org/10.1016/j.molcel.2010.12.013>
- 714 40. Lu, J. Q., Cheng, K. Y., Zhang, B., Xu, H., Cao, Y. Z., Guo, F., Feng, X. D., & Xia,
715 Q. (2015). Novel mechanisms for superoxide-scavenging activity of human
716 manganese superoxide dismutase determined by the K68 key acetylation site. *Free*
717 *Radical Biology and Medicine*, 85, 114-126.
718 <https://doi.org/10.1016/j.freeradbiomed.2015.04.011>
- 719 41. Zhang, X. F., Ren, X. Q., Zhang, Q., Li, Z. Y., Ma, S. P., Bao, J. T., Li, Z. Y., Bai,
720 X., Zheng, L. J., Zhang, Z., Shang, S. J., Zhang, C., Wang, C. G., Cao, L., Wang,
721 Q. S., & Ji, J. G. (2016). PGC-1 alpha/ERR alpha-Sirt3 Pathway Regulates DAergic
722 Neuronal Death by Directly Deacetylating SOD2 and ATP Synthase beta.
723 *Antioxidants & Redox Signaling*, 24(6), 312-328.
724 <https://doi.org/10.1089/ars.2015.6403>
- 725 42. Lin, C. T., Tseng, W. C., Hsiao, N. W., Chang, H. H., & Ken, C. F. (2009).
726 Characterization, molecular modelling and developmental expression of zebrafish
727 manganese superoxide dismutase. *Fish & Shellfish Immunology*, 27(2), 318-324.
728 <https://doi.org/10.1016/j.fsi.2009.05.015>
- 729 43. Yang, M. K., Huang, H., & Ge, F. (2019). Lysine Propionylation is a Widespread
730 Post-Translational Modification Involved in Regulation of Photosynthesis and
731 Metabolism in Cyanobacteria. *International Journal of Molecular Sciences*, 20(19).
732 <https://doi.org/Artn 4792 10.3390/Ijms20194792>
- 733 44. Michishita, E., Park, J. Y., Burneskis, J. M., Barrett, J. C., & Horikawa, I. (2005).
734 Evolutionarily conserved and nonconserved cellular localizations and functions of
735 human SIRT proteins. *Molecular Biology of the Cell*, 16(10), 4623-4635.
736 <https://doi.org/10.1091/mbc.E05-01-0033>
- 737 45. Bause, A. S., & Haigis, M. C. (2013). SIRT3 regulation of mitochondrial oxidative
738 stress. *Experimental Gerontology*, 48(7), 634-639.
739 <https://doi.org/10.1016/j.exger.2012.08.007>
- 740 46. Wang, X. Q., Shao, Y., Ma, C. Y., Chen, W., Sun, L., Liu, W., Zhang, D. Y., Fu, B.
741 C., Liu, K. Y., Jia, Z. B., Xie, B. D., Jiang, S. L., Li, R. K., & Tian, H. (2014).
742 Decreased SIRT3 in aged human mesenchymal stromal/stem cells increases cellular

- 743 susceptibility to oxidative stress. *Journal of Cellular and Molecular Medicine*,
744 18(11), 2298-2310. <https://doi.org/10.1111/jcmm.12395>
- 745 47. Garrity, J., Gardner, J. G., Hawse, W., Wolberger, C., & Escalante-Semerena, J. C.
746 (2007). N-Lysine propionylation controls the activity of propionyl-CoA synthetase.
747 *Journal of Biological Chemistry*, 282(41), 30239-30245.
748 <https://doi.org/10.1074/jbc.M704409200>
- 749 48. Nahomi, R. B., Nandi, S. K., Rakete, S., Michel, C., Fritz, K. S., & Nagaraj, R. H.
750 (2020). Lysine malonylation and propionylation are prevalent in human lens
751 proteins. *Experimental Eye Research*, 190. <https://doi.org/Art107864>
752 [10.1016/j.exer.2019.107864](https://doi.org/10.1016/j.exer.2019.107864)
- 753 49. Zhang, S. J., Li, Y. F., Wang, G. E., Tan, R. R., Tsoi, B., Mao, G. W., Zhai, Y. J.,
754 Cao, L. F., Chen, M., Kurihara, H., Wang, Q., & He, R. R. (2015). Caffeine
755 ameliorates high energy diet-induced hepatic steatosis: sirtuin 3 acts as a bridge in
756 the lipid metabolism pathway. *Food & Function*, 6(8), 2578-2587.
757 <https://doi.org/10.1039/c5fo00247h>
- 758 50. Yu, W., Qin, J. J., Chen, C. J., Fu, Y. C., & Wang, W. (2018). Moderate calorie
759 restriction attenuates age-associated alterations and improves cardiac function by
760 increasing SIRT1 and SIRT3 expression. *Molecular Medicine Reports*, 18(4), 4087-
761 4094. <https://doi.org/10.3892/mmr.2018.9390>
- 762 51. Kong, X. X., Wang, R., Xue, Y., Liu, X. J., Zhang, H. B., Chen, Y., Fang, F., &
763 Chang, Y. S. (2010). Sirtuin 3, a New Target of PGC-1 alpha, Plays an Important
764 Role in the Suppression of ROS and Mitochondrial Biogenesis. *Plos One*, 5(7).
765 <https://doi.org/ARTN1170710.1371/journal.pone.0011707>
- 766 52. Yoon, S. P., & Kim, J. (2016). Poly(ADP-ribose) polymerase 1 contributes to
767 oxidative stress through downregulation of sirtuin 3 during cisplatin nephrotoxicity.
768 *Anat Cell Biol*, 49(3), 165-176. <https://doi.org/10.5115/acb.2016.49.3.165>
- 769 53. Kim, S., Piao, S., Lee, I., Nagar, H., Choi, S. J., Shin, N., Kim, D. W., Shong, M.,
770 Jeon, B. H., & Kim, C. S. (2020). CR6 interacting factor 1 deficiency induces
771 premature senescence via SIRT3 inhibition in endothelial cells. *Free Radic Biol*
772 *Med*, 150, 161-171. <https://doi.org/10.1016/j.freeradbiomed.2020.02.017>

- 773 54. Saint-Georges-Chaumet, Y., & Edeas, M. (2016). Microbiota-mitochondria inter-
774 talk: consequence for microbiota-host interaction. *Pathogens and Disease*, 74(1),
775 ftv096. <https://doi.org/10.1093/femspd/ftv096>
- 776 55. Emre, Y., & Nubel, T. (2010). Uncoupling protein UCP2: When mitochondrial
777 activity meets immunity. *Febs Letters*, 584(8), 1437-1442.
778 <https://doi.org/10.1016/j.febslet.2010.03.014>
- 779 56. Conlon, M. A., & Bird, A. R. (2015). The Impact of Diet and Lifestyle on Gut
780 Microbiota and Human Health. *Nutrients*, 7(1), 17-44.
781 <https://doi.org/10.3390/nu7010017>
- 782 57. Hevia, A., Bernardo, D., Montalvillo, E., Al-Hassi, H. O., Fernandez-Salazar, L.,
783 Garrote, J. A., Milani, C., Ventura, M., Arranz, E., Knight, S. C., Margolles, A., &
784 Sanchez, B. (2015). Human colon-derived soluble factors modulate gut microbiota
785 composition. *Frontiers in Oncology*, 5. https://doi.org/Unsp_96_10.3389/Fonc.2015.00086
- 787 58. Ma, Y., Chai, H., Ding, Q. C., Qian, Q. Y., Yan, Z. Y., Ding, B., Dou, X. B., & Li,
788 S. T. (2019). Hepatic SIRT3 Upregulation in Response to Chronic Alcohol
789 Consumption Contributes to Alcoholic Liver Disease in Mice. *Frontiers in*
790 *Physiology*, 10. https://doi.org/Artn_1042_10.3389/Fphys.2019.01042
- 791 59. Palacios, O. M., Carmona, J. J., Michan, S., Chen, K. Y., Manabe, Y., Ward, J. L.,
792 Goodyear, L. J., & Tong, Q. (2009). Diet and exercise signals regulate SIRT3 and
793 activate AMPK and PGC-1 alpha in skeletal muscle. *Aging-Us*, 1(9), 771-783.
794 https://doi.org/Doi_10.18632/Aging.100075
- 795 60. Fritz, K. S., Green, M. F., Petersen, D. R., & Hirschey, M. D. (2013). Ethanol
796 Metabolism Modifies Hepatic Protein Acylation in Mice. *Plos One*, 8(9).
797 https://doi.org/ARTN_e75868_10.1371/journal.pone.0075868
- 798 61. Wongkittichote, P., Mew, N. A., & Chapman, K. A. (2017). Propionyl-CoA
799 carboxylase - A review. *Molecular Genetics and Metabolism*, 122(4), 145-152.
800 <https://doi.org/10.1016/j.ymgme.2017.10.002>
- 801 62. Xu, J. Y., Xu, Y., Xu, Z., Zhai, L. H., Ye, Y., Zhao, Y. M., Chu, X. H., Tan, M. J.,
802 & Ye, B. C. (2018). Protein Acylation is a General Regulatory Mechanism in

- 803 Biosynthetic Pathway of Acyl-CoA-Derived Natural Products. *Cell Chemical*
804 *Biology*, 25(8), 984-+. <https://doi.org/10.1016/j.chembiol.2018.05.005>
- 805 63. McElhanon, B. O., McCracken, C., Karpen, S., & Sharp, W. G. (2014).
806 Gastrointestinal Symptoms in Autism Spectrum Disorder: A Meta-analysis.
807 *Pediatrics*, 133(5), 872-883. <https://doi.org/10.1542/peds.2013-3995>
- 808 64. Wang, L., Conlon, M. A., Christophersen, C. T., Sorich, M. J., & Angley, M. T.
809 (2014). Gastrointestinal microbiota and metabolite biomarkers in children with
810 autism spectrum disorders. *Biomarkers in Medicine*, 8(3), 331-344.
811 <https://doi.org/10.2217/bmm.14.12>
- 812 65. Strati, F., Cavalieri, D., Albanese, D., De Felice, C., Donati, C., Hayek, J., Jousson,
813 O., Leoncini, S., Renzi, D., Calabro, A., & De Filippo, C. (2017). New evidences
814 on the altered gut microbiota in autism spectrum disorders. *Microbiome*, 5.
815 <https://doi.org/ARTN 24 10.1186/s40168-017-0242-1>
- 816 66. Finegold, S. M., Dowd, S. E., Gontcharova, V., Liu, C. X., Henley, K. E., Wolcott,
817 R. D., Youn, E., Summanen, P. H., Granpeesheh, D., Dixon, D., Liu, M., Molitoris,
818 D. R., & Green, J. A. (2010). Pyrosequencing study of fecal microflora of autistic
819 and control children. *Anaerobe*, 16(4), 444-453.
820 <https://doi.org/10.1016/j.anaerobe.2010.06.008>
- 821 67. Nina, G., & David, R. (2017). Autism Spectrum Disorder and Inflammatory Bowel
822 Disease: Determination of a Pathophysiologic Link and Special Considerations for
823 a Unique Patient Population. *Inflamm Bowel Dis*, 23, S15-S15. <Go to
824 ISI>://WOS:000393902100045
- 825 68. de Keyzer, Y., Valayannopoulos, V., Benoist, J. F., Batteux, F., Lacaille, F., Hubert,
826 L., Chretien, D., Chadeveau-Vekemans, B., Niaudet, P., Touati, G., Munnich, A.,
827 & de Lonlay, P. (2009). Multiple OXPHOS Deficiency in the Liver, Kidney, Heart,
828 and Skeletal Muscle of Patients With Methylmalonic Aciduria and Propionic
829 Aciduria. *Pediatr Res*, 66(1), 91-95. [https://doi.org/Doi](https://doi.org/Doi 10.1203/Pdr.0b013e3181a7c270)
830 [10.1203/Pdr.0b013e3181a7c270](https://doi.org/Doi 10.1203/Pdr.0b013e3181a7c270)
- 831 69. Gallego-Villar, L., Perez-Cerda, C., Perez, B., Abia, D., Ugarte, M., Richard, E., &
832 Desviat, L. R. (2013). Functional characterization of novel genotypes and cellular

- 833 oxidative stress studies in propionic acidemia. *Journal of Inherited Metabolic*
834 *Disease*, 36(5), 731-740. <https://doi.org/10.1007/s10545-012-9545-3>
- 835 70. Gallego-Villar, L., Rivera-Barahona, A., Cuevas-Martin, C., Guenzel, A., Perez, B.,
836 Barry, M. A., Murphy, M. P., Logan, A., Gonzalez-Quintana, A., Martin, M. A.,
837 Medina, S., Gil-Izquierdo, A., Cuezva, J. M., Richard, E., & Desviat, L. R. (2016).
838 In vivo evidence of mitochondrial dysfunction and altered redox homeostasis in a
839 genetic mouse model of propionic acidemia: Implications for the pathophysiology
840 of this disorder. *Free Radical Biology and Medicine*, 96, 1-12.
841 <https://doi.org/10.1016/j.freeradbiomed.2016.04.007>
- 842 71. Rawls, J. F., Mahowald, M. A., Ley, R. E., & Gordon, J. I. (2006). Reciprocal gut
843 microbiota transplants from zebrafish and mice to germ-free recipients reveal host
844 habitat selection. *Cell*, 127(2), 423-433. <https://doi.org/10.1016/j.cell.2006.08.043>
- 845 72. Driever, W., & Rangini, Z. (1993). Characterization of a cell line derived from
846 zebrafish (*Brachydanio rerio*) embryos. *In Vitro Cell Dev Biol Anim*, 29A(9), 749-
847 754. <https://doi.org/10.1007/BF02631432>
- 848 73. Zhang, Z., Ran, C., Ding, Q. W., Liu, H. L., Xie, M. X., Yang, Y. L., Xie, Y. D.,
849 Gao, C. C., Zhang, H. L., & Zhou, Z. G. (2019). Ability of prebiotic polysaccharides
850 to activate a HIF1 alpha-antimicrobial peptide axis determines liver injury risk in
851 zebrafish. *Communications Biology*, 2. [https://doi.org/10.1038/S42003-](https://doi.org/10.1038/S42003-019-0526-Z)
852 [019-0526-Z](https://doi.org/10.1038/S42003-019-0526-Z)

853 **Acknowledgments**

854 This work was supported by the National Natural Science Foundation of China (NSFC
855 31925038, 31972807, 31872584, 31802315) and the National Key R&D Program of
856 China (2018YFD0900400) and the National Natural Science Foundation of China
857 (NSFC 31802315, 31760762, 31872584 and 31702354) funded this work for grants to
858 Dr. Zhigang Zhou, and NIBIO's STIM China grant (Grant No. 51133) to Dr Jihong Liu
859 Clarke. The authors thank Prof. Nicholas Clarke for linguistic proof reading.

860 **Author contributions**

861 Z.Z.G. designed the research. D.Q.W and R.C. wrote the paper, and Z.Z.G. gave
862 conceptual advice for the paper. J.L.C. reviewed and helped to revise the manuscript.
863 D.Q.W performed experiments and acquired data. Z.Z. and Y.L. assisted in the *q*PCR,
864 western blot, gut microbiota analysis and *si*RNA knockdown experiments. L.H.L. and
865 H.Q. participated in zebrafish husbandry and sampling. R.C., Y.Y.L. and Z.Z. co-
866 analyzed and discussed the results. All authors read and approved the final manuscript.

867 **Competing interests:** The authors declare no competing interests.